J. Paleont., 81(4), 2007, pp. 607–631

0022-3360/07/0081-607$03.00

MORPHOLOGY, ONTOGENY, AND PHYLOGENETICS OF THE GENUS *POSEIDONAMICUS* (OSTRACODA: THAEROCYTHERINAE)

GENE HUNT

Department of Paleobiology, National Museum of Natural History, Smithsonian Institution, Washington, DC 20013-7012. ⟨hunte@si.edu⟩

ABSTRACT—The ostracode genus *Poseidonamicus* has been widespread and abundant in deep-sea sediments since the Eocene. Despite its prominent role in a number of evolutionary studies, species identification in this genus is often difficult and phylogenetic relationships among its species are not well understood. Here I present the findings from a comprehensive study of this genus with the purpose of discovering novel phylogenetic characters and clarifying species relationships. I briefly describe the adult carapace and trace some of the major morphological changes that occur over the last several instars. I focus particular attention on the arrangement of fossae in the reticulate mesh; these features have been shown in other ostracodes to correspond to underlying epidermal cells. I describe the development of fossae in the region posterior to the adductor muscle scars, and hypothesize a sequence of specific cell divisions to account for the addition of fossae over ontogeny.

Phylogenetic characters were derived from many different types of characters, including aspects of carapace shape, the presence and location of pores, characteristics of specific ridges and spines, and the relative position of homologous fossae in the reticulum. A parsimony analysis of 42 characters and 40 operational taxonomic units (36 ingroup and four outgroup) resulted in a set of optimal trees whose strict consensus is relatively well resolved, well supported, and generally consistent with the order in which taxa appear in the fossil record. The monophyly of *Poseidonamicus* is supported, as is the monophyly of all deep-sea members of this genus. Within the clade of deep-sea *Poseidonamicus*, several subgroups are recovered with varying levels of character support. In addition to providing a general framework for understanding morphological evolution in this genus, the results of this phylogenetic analysis have two specific implications for the evolution of sightedness in this genus. First, because *Poseidonamicus ocularis* is nested deeply within a clade of entirely deep-sea species, its putatively ocular features are probably not related to vision. Second, there has likely been just a single transition from sighted to blind in *Poseidonamicus*, coincident with its colonization of the deep sea. No support is found for the recent suggestion that sighted shallow-water dwelling *Poseidonamicus* species may have evolved from blind deep-sea ancestors, although data from additional taxa will be necessary to test this hypothesis more fully.

INTRODUCTION

THE GENUS *Poseidonamicus* was erected by Benson (1972) to accommodate several deep-sea thaerocytherine ostracode species that share a unique style of surface reticulation. Of the 16 described species currently assigned to this genus (Table 1), 14 are found exclusively in deep-sea sediments greater than 1 km in depth, where the genus has been common and geographically widespread since the Eocene. The remaining two species are known from modern continental shelf sediments from a few localities in the Southern Hemisphere (Whatley and Dingle, 1989; Dingle, 2003a).

Several workers have taken advantage of the relatively high abundance, distinctive morphology, and continuous deep-sea record of *Poseidonamicus* to analyze evolutionary patterns in this genus. Whatley and colleagues (Whatley et al., 1983; Whatley, 1985) documented its phylogenetic history in the southwest Pacific Ocean, an area they considered a center of origin and diversity for this genus. These authors also proposed relationships among seven species within the genus, primarily based on characteristics of the reticulum. Several other studies have investigated more specific aspects of *Poseidonamicus* morphology. Benson (1983) and Benson and Peypouquet (1983) considered carapace evolution from a biomechanical perspective, and the evolution of sightedness was discussed by Whatley and Dingle (1989), and more recently by Dingle (2002, 2003b).

Despite considerable interest in the processes shaping evolution in this genus, phylogenetic relationships among its species are not well understood. Moreover, while *Poseidonamicus* is readily discriminated from other deep-sea genera, species differences within the genus are often subtle. Although this problem is common among ostracodes, species identification within *Poseidonamicus* is difficult enough to be seen as an impediment to paleobiological and paleoceanographic analysis (Ayress et al., 1997). In this paper, I explore the morphology, ontogeny, and phylogenetic history of the genus *Poseidonamicus*, in order to: 1) discover characters that allow for reliable identification of species and clades, and 2) provide a robust evolutionary framework for morphological and paleoceanographic studies of this genus.

MORPHOLOGY OF *POSEIDONAMICUS*

Overview.—This section gives a brief overview of the carapace morphology of *Poseidonamicus*; readers are referred to Benson (1972) and Whatley et al. (1986) for a complete diagnosis and description of the genus. *Poseidonamicus* is subquadrate in lateral view, with a meshlike surface reticulum that varies from coarse to nearly smooth. This reticulum is composed of skeletal ridges called muri that bound excavate compartments called fossae (Sylvester-Bradley and Benson, 1971). The reticulum is divided into anterior and posterior fields by what Benson (1972) termed the mural loop (Fig. 1.1). Fossae in the posterior field are polygonal and the muri are often vertically aligned. In contrast, anterior field fossae are distinctly rounded and separated by muri that are lower, broader, and more uniform in height than those in the posterior.

Poseidonamicus valves have a prominent ventrolateral ridge (VR; see Table 2 for anatomical abbreviations used in this paper) that terminates posteriorly in a prominent spine that protrudes posterolaterally. The dorsal ridge (DR) may be continuous or interrupted. In most species, the DR is prominent, but in some it is reduced in thickness and/or anterior-posterior extent. The anterior margin of each valve has a single row of approximately 15–20 denticles; the posterior margin bears fewer denticles and several larger spines. The anterior, ventral, and posterior edges of the valves are lined with marginal rims that are smooth, flat, and approximately parallel to the commissure. Right and left valves are equal in length, but the left valve overlaps the right immediately anterior to the anterior cardinal angle (ACA) and immediately posterior to the posterior cardinal angle (PCA). Valves are perforated by numerous pores, generally murate, and of both simple and sieve type. Hingement is holamphidont, with a stepped anterior tooth and a subtly lobate posterior tooth in right valves. In left valves, the medial bar is smooth, as is the medial hinge element.

Fossae arrangement.—One of the most striking aspects of *Poseidonamicus* morphology is the regular arrangement of fossae in the reticulum. In several similarly reticulate cytheroidean species, it has been shown that each fossa corresponds to an underlying

TABLE 1—Formally described species currently assigned to the genus *Poseidonamicus*. 'OTU prefix' refers to the naming of operational taxonomic units in the current study; see text for details.

Species	Reference	OTU prefix
Poseidonamicus major	Benson, 1972	maj
Poseidonamicus minor	Benson, 1972	min
Poseidonamicus pintoi	Benson, 1972	pin
Poseidonamicus nudus	Benson, 1972	nud
Poseidonamicus riograndensis	Benson and Peypouquet, 1983	rio
Poseidonamicus miocenicus	Benson and Peypouquet, 1983	mio
Poseidonamicus anteropunctatus	Whatley et al., 1986	ant
Poseidonamicus ocularis	Whatley et al., 1986	ocu
Poseidonamicus praenudus	Whatley et al., 1986	pra
Poseidonamicus punctatus	Whatley et al., 1986	pun
Poseidonamicus robustus	Whatley et al., 1986	rob
Poseidonamicus rudis	Whatley et al., 1986	rud
Poseidonamicus pseudorobustus	Coles and Whatley, 1989	pse
Poseidonamicus panopsus	Whatley and Dingle, 1989	pan
Poseidonamicus dinglei	Boomer, 1999	din
Poseidonamicus whatleyi	Dingle, 2003a	—

epidermal cell (Okada, 1981, 1982a). Consequently, reticulate ostracodes offer a rare opportunity to infer aspects of cellular anatomy in fossil populations. Many individual fossae can be recognized in all species of *Poseidonamicus*, and even related genera such as *Bradleya* Hornibrook, 1952. Such conservation of fossae arrangement across related genera is not uncommon in comparative studies (Liebau, 1971, 1991; Benson, 1972; Irizuki, 1993, 1996).

In order to facilitate comparison among specimens, I used a coding scheme to label a subset of the fossae in the reticulum (Fig. 1.2). The fossae most readily identifiable across species are located in the region immediately posterior to the adductor scars between the dorsal and ventrolateral ridges, and in the area abutting the anterior marginal rim (Fig. 1.2). As homology was sometimes uncertain in the remaining regions of the reticulum, they were not incorporated into the present coding system. Nevertheless, further comparative work may eventually clarify some of these ambiguities.

This coding scheme divided the reticulum into approximately vertical columns of fossae. Each column was assigned a letter, and fossae within a column were numbered consecutively from ventral to dorsal. Columns posterior to the mural loop were labeled consecutively from A to D (Fig. 1.2). The column of fossae containing the mural loop was labeled 'M,' and the fossae abutting the marginal rim were given the descriptive prefix 'AR' for 'anterior rim.'

Many similar coding schemes have been used to label fossae in other reticulate ostracodes (e.g., Liebau, 1971; Benson, 1972; Irizuki, 1994, 1996). These coding schemes are not meant to imply biological differences between fossae from different columns or rows (for example, fossae in column A vs. fossae in column B). Rather, these labeling schemes are useful for breaking down complex patterns into simpler units, facilitating the recognition of similarities and differences among specimens.

Primary and secondary reticulation.—The meshwork of skeletal ridges outlining the fossae in Figure 1 is referred to as primary reticulation. Some specimens, especially relatively less robust forms, have secondary reticulation superimposed upon this primary mesh (Sylvester-Bradley and Benson, 1971). In all species of *Poseidonamicus*, overall robustness increases over ontogeny, causing a concomitant decrease in the prevalence of secondary reticulation. In most species in the genus, secondary reticulation is prevalent in early instars, present but less dominant in later juvenile stages, and completely absent in adults. The only populations to show extensive secondary reticulation as adults are from species with a reduced reticulum, such as *P. nudus* Benson, 1972, or those from great depth (>4 km) living in conditions unfavorable to calcium carbonate deposition.

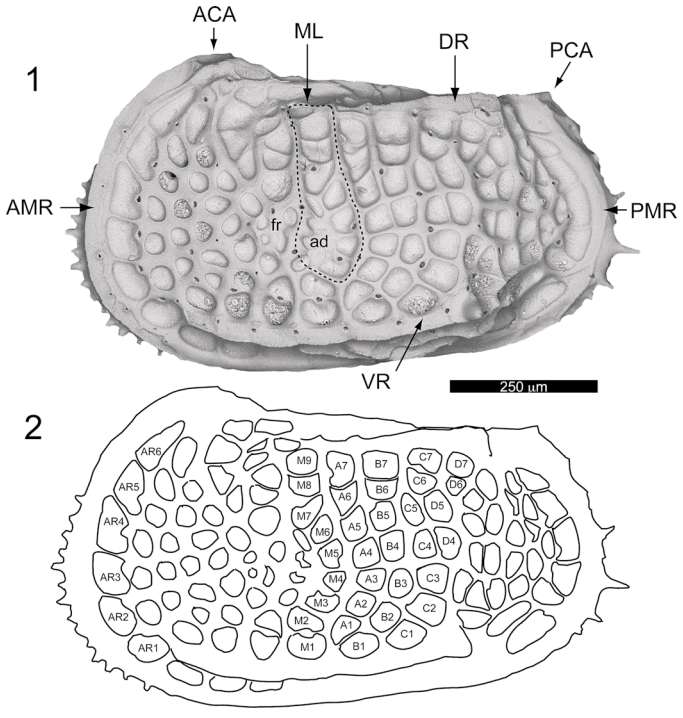

FIGURE 1—Morphology of adult male *Poseidonamicus pintoi* Benson, 1972 from the Quaternary of the North Atlantic (OTU pin-Q234). *1,* SEM image of USNM 527093; see Table 2 for description of abbreviations. *2,* Line drawing of the same specimen with fossae labeled according to coding scheme described in the text.

TABLE 2—Anatomical abbreviations used in the current study.

Abbreviation	Character
VR	Ventrolateral ridge
DR	Dorsal ridge
AMR	Anterior marginal rim
PMR	Posterior marginal rim
ML	Mural loop
ACA	Anterior cardinal angle
PCA	Posterior cardinal angle
IL	Inner lamella
LV	Left valve
RV	Right valve
ad	Adductor muscle scars
fr	Frontal muscle scars

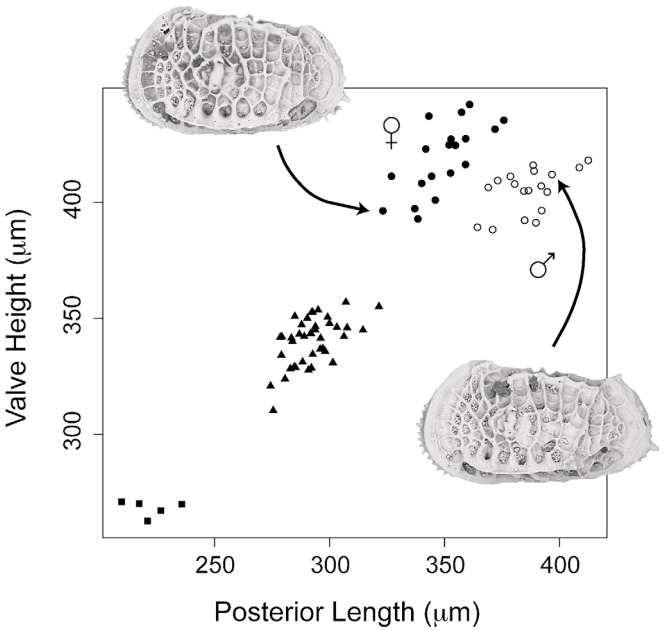

FIGURE 2—Biometric clusters of instars and sexes in *Poseidonamicus riograndensis* Benson *in* Benson and Peypouquet, 1983 from a single sample from the early Miocene (DSDP 526A 22/1/124–130). Posterior length was measured from posterior edge of the mural loop to the posterior extremity of the valve; valve height was measured at the adductor muscle scars. Open circles = males, filled circles = females, triangles = A-1 instar, squares = A-2 instar.

ONTOGENY

Instar and sex differences.—Instars in *Poseidonamicus* are usually biometrically discrete in populations with sample sizes large enough for statistical analysis (Hunt and Chapman, 2001). One example of a population with clear instar size clusters is shown in Figure 2. In this genus, linear dimensions increase by approximately 25% with each juvenile molt, and by a slightly lesser amount in the final molt to the adult stage. The carapace of *Poseidonamicus*, like that of most cytheroidean ostracodes, is sexually dimorphic. In order to accommodate their bulky copulatory apparatus, males are relatively elongate in the posterior region (Maddocks, 1992). As a result, sexes can be distinguished by plotting the length of the posterior portion of the valve (from the mural loop to the posterior extreme) versus valve height (Fig. 2). Sex ratios are often female-skewed in *Poseidonamicus*, a pattern that is commonly reported in other ostracode groups (van Morkhoven, 1962; Cohen and Morin, 1990; Chaplin et al., 1994).

Biometric clustering of instars facilitates the identification of features other than body size that differ consistently among instar stages. Such features are useful for inferring instar assignments in samples too small for statistical size clusters to be determined reliably. A list of characters that vary consistently with instar in *Poseidonamicus* is given in Table 3. Features of the anterior marginal rim, ventrolateral ridge, and anterior rim fossae are sufficient to uniquely characterize the A-4 through A-1 juvenile instars. Adults differ from A-1 juveniles by their markedly larger hinge elements and substantially wider inner lamellae. In addition to the features listed in Table 3, each juvenile instar may also be recognized by its characteristic fossae arrangement in the posterior field, as I discuss in the next section. Neither the features listed in Table 3 nor the details of fossae arrangement were ever observed to conflict with instar assignments implied by biometric clustering. As a result, of the over 3,000 *Poseidonamicus* specimens studied, instar assignment was ambiguous for only a few individuals.

Fossae patterns by instar.—The number of fossae in the reticulum increases with each juvenile molt. This progression is shown for posterior field fossae in *Poseidonamicus riograndensis* Benson *in* Benson and Peypouquet, 1983 instars A-3 through A-1 (Fig. 3). This species' lack of secondary reticulation in juvenile stages makes it particularly useful for illustrating the primary mural mesh outlining each fossa. Because of their correspondence to underlying epidermal cells, new fossae added with each molt are interpreted to arise from the division of the epidermal cells underlying preexisting fossae (Okada, 1981). This interpretation is consistent with several aspects of how fossae multiply over ontogeny. Typically, a single large fossa is replaced in the next instar with two proportionately smaller fossae in the same region of the reticulum (Fig. 3). Anatomical landmarks such as muscle scars, pores, and ridges help to identify corresponding regions of the reticulum between instars, allowing one to infer which fossae (or more precisely, which corresponding epidermal cells) have divided from one instar to the next.

In addition to showing the increase in the number of fossae through three molt stages, the fossae labeling in Figure 3 presents a hypothesized sequence of cell divisions. This labeling is best understood by considering each fossa of the A-1 instar and working backwards through ontogeny. If a fossa in the A-2 instar does not divide between the A-2 and A-1 instars, this fossa is given the same name as its homologue in A-1. If the fossa does divide, it is labeled with the combined names of its daughter fossae in A-1. For example, according to this hypothesis, fossae A1 and B1 in the A-1 instar are daughter cells resulting from the division of a single fossa in the previous instar. This parent fossa to A1 and B1 is therefore labeled A1B1 (Fig. 3.6, 3.9). This procedure is then repeated for earlier instar transitions. In total, five cell divisions are inferred to occur between instars A-3 and A-2 and six between the A-2 and A-1 instars (Table 4). Because the A-1 and adult stages have exactly the same arrangement of fossae, no cell divisions occur during the molt separating these instars. Okada (1981) reported the same constancy of fossae arrangement between the A-1 and adult stages of the trachyleberidid ostracode *Bicornucythere bisanensis* (Okubo, 1975).

With one exception, the same sequence of cell divisions summarized in Figure 3 and Table 4 seems to occur in all species of *Poseidonamicus* that I have examined. This exception occurs in

TABLE 3—Morphological features useful for assigning *Poseidonamicus* specimens to instars. AR = anterior row; otherwise, see Table 2 for anatomical abbreviations.

Trait	Instar				Adult
	A-4	A-3	A-2	A-1	
AMR pores	Absent	Present	Present	Present	Present
VR	Absent except for posterior spine	Absent or present only in posterior	Complete	Complete	Complete
# pores on the VR	—	—	3	7	7
# AR fossae in LV	—	5	6	6	6
# AR fossae in LV with pores	—	2	4	6	6
Hinge elements	Small	Small	Small	Small	Large
Inner lamella	Narrow	Narrow	Narrow	Narrow	Wide

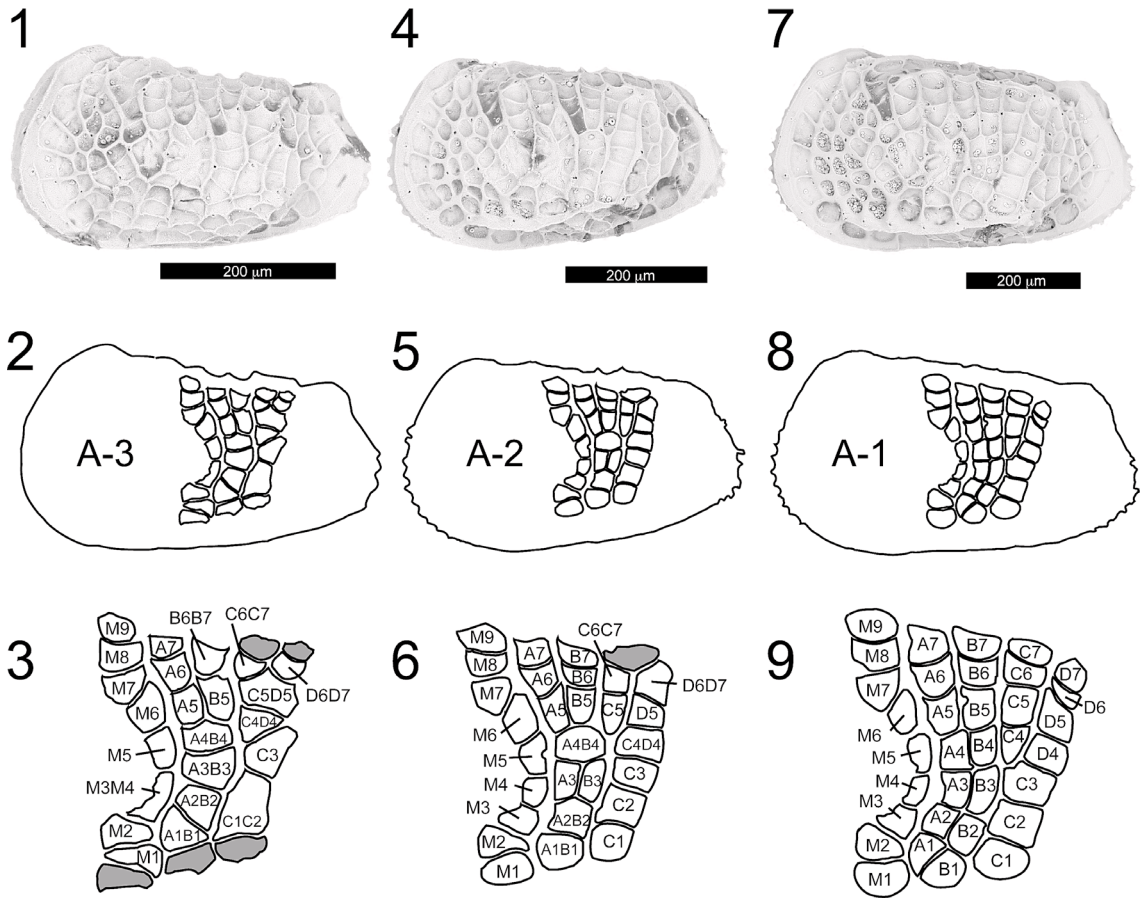

FIGURE *3*—Ontogeny of fossae arrangement for instars A-3 through A-1 in *Poseidonamicus riograndensis*. For each instar, an SEM image, outline drawing, and close-up of the labeled fossae of the posterior field is given; shaded fossae are inferred to be subsumed into the developing dorsal and ventral ridges. See text for details. *1–3,* A-3 instar. *4–6,* A-2 instar. *7–9,* A-1 instar.

the species *P. dinglei* Boomer, 1999, *P. anteropunctatus* Whatley et al., 1986, *P. punctatus* Whatley et al., 1986, *P. praenudus* Whatley et al., 1986, and *P. nudus*. These species have two smaller fossae in the position usually occupied by a single large C3 fossa in all other *Poseidonamicus* species (compare Fig. 4.1, 4.3). This extra fossa first appears in the A-1 instar, presumably the product of a novel division in the epidermal cell underlying the C3 fossa. Because this extra fossa is invariably correlated with the absence of the sieve pore that is normally found near anterodorsal corner of fossa C3 (Fig. 4.1), it is likely that these two states are developmentally coupled.

TABLE *4*—Cell divisions occurring during the last two juvenile molts in *Poseidonamicus riograndensis*. The cell divisions are inferred on the basis of fossae arrangement patterns characteristic of each instar. See Figure 3 for an illustration of these fossae. 'Direction of division' refers to the anatomical direction separating the two daughter cells: dv = dorsal-ventral, ap = anterior-posterior.

Instar Transition	Parent Fossa	Direction of Division
A-3 to A-2	M3M4	dv
	A3B3	ap
	B6B7	dv
	C1C2	dv
	C5D5	ap
A-2 to A-1	A1B1	ap
	A2B2	ap
	A4B4	ap
	C4D4	ap
	C6C7	dv
	D6D7	dv
A-1 to adult		no divisions

Variant fossae arrangements.—Despite its overall consistency among lineages, fossae arrangement often shows some within-population variation. Some variant individuals deviate from the typical fossae arrangement across a broad region of the valve. It seems likely that these variants result from a genetic or environmental perturbation that causes a large disruption across the region in which it occurs. Often, however, deviations are more local in extent, and seem to result from perturbations of specific cell divisions events. For example, if an area typically occupied by two fossae instead has a single larger fossa, this would suggest that the epidermal cell underlying the single larger fossa failed to divide in its usual manner. This interpretation is strengthened if an ontogenetic study indicates that these two fossae are normally daughter cells produced by the same cell division. Another example concerns the extra C3 fossa that is typical of *P. dinglei* and a few other lineages. This morphology appears to be fixed within this group of species, but it also occurs at low frequency (generally less than 5%) in most other species within the genus (Fig. 4.2).

When interpreting variation in fossae arrangement, care must be taken to account for secondary reticulation obscuring the primary reticulate mesh, especially in younger juvenile stages and less robust species. Secondary reticulation can usually be distinguished from primary reticulation by its lower elevation and more variable expression. A different complication arises when one or more muri are very reduced. In such cases, casual inspection might suggest the presence of a large undivided fossa in a region

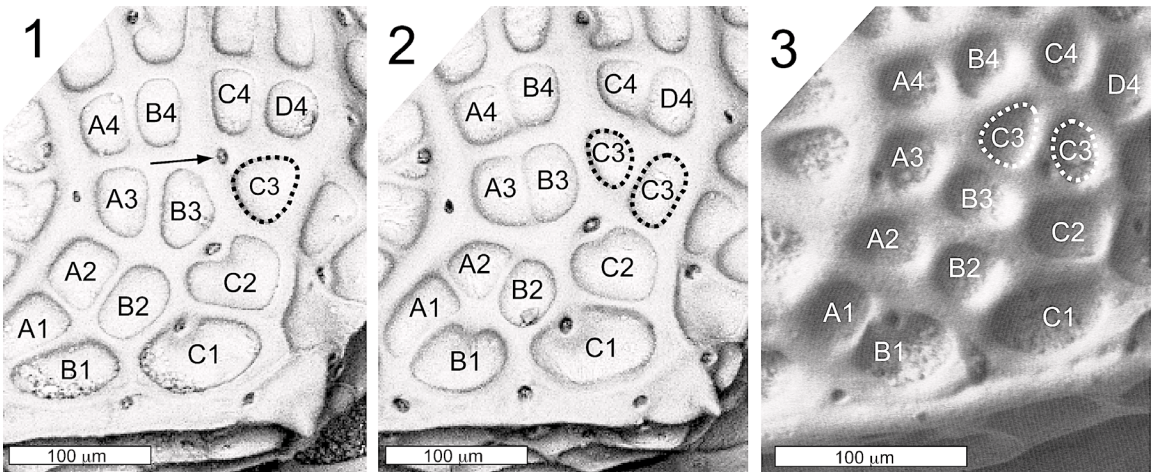

FIGURE 4—Undivided and divided C3 fossa morphologies. *1, 2,* Within-population variation in a population of *Poseidonamicus pintoi*. Both specimens shown are A-1 individuals from the same OTU (pin-Q234). *1,* Individual with the fossae pattern typical for this species. Arrow points to the pore absent in individuals with an extra C3 fossa. *2,* Individual with an extra fossa, attributable to an extra cell division of the epidermal cell underlying the C3 fossa. *3,* Divided C3 fossa in adult *P. punctatus* (OTU pun-Q1). In all three figures, dotted lines surround C3 fossa or its presumed daughter fossae. See text for details.

of the reticulum where normally two fossae reside. Nevertheless, close examination will usually reveal a trace of the separating mura. In addition, the presence of a pore in the middle of what appears to be a single large fossa also indicates the presence of two separate fossae because pores perforate the valve at the junction of epidermal cells, rather than tunneling through the middle of individual cells (Okada, 1982b; Hanai and Ikeya, 1991).

Development of dorsal and ventrolateral ridges.—The development of the dorsal and ventrolateral ridges can be seen in Figure 3. In the A-3 instar, the VR is undeveloped although its terminating spine is generally present (this spine is somewhat worn in the specimen in Fig. 3.1). Anterior to this spine are a series of dorsoventrally narrow fossae that seem to be replaced by the VR in subsequent instars (these fossae are filled in grey in Fig. 3.3). This interpretation is supported by observations of rare individuals with a discontinuous VR. In these individuals, a single dorsoventrally narrow fossa can be seen in place of the missing VR segment.

A similar process seems to generate the dorsal ridge. Dorsal to fossa D6D7 in the A-3 instar, there is a small fossa that is replaced in the subsequent instar by a smooth flat region. This smooth region eventually forms the posterior termination of the DR. Similarly, there is an elongate fossa dorsal to C6C7 in the A-2 instar that is not recognizable in the following instar. In A-2 individuals with a well-developed DR (such as those from the robust species *P. minor* Benson, 1972), this particular fossa is not visible, consistent with the interpretation that it is subsumed into the developing DR.

These observations strongly suggest that the dorsal and ventrolateral ridges have a different developmental basis than all other muri in the reticulum. Typically, muri form at the junction of fossae, outlining the underlying epidermal cells. In contrast, the DR and VR are each underlain by a row of fossae that are evenly filled with skeletal material. It is currently unknown to what extent developmental differences between muri and ridges influence how these structures vary and evolve.

PHYLOGENETIC ANALYSIS

Material.—I examined samples spanning the entire geographic and stratigraphic extent of the genus *Poseidonamicus* (Fig. 5, App. 1). Hundreds of samples and thousands of individual ostracodes were studied. Most specimens were from the large deep-sea Ostracoda collections of the National Museum of Natural History (Washington, DC) and the Natural History Museum

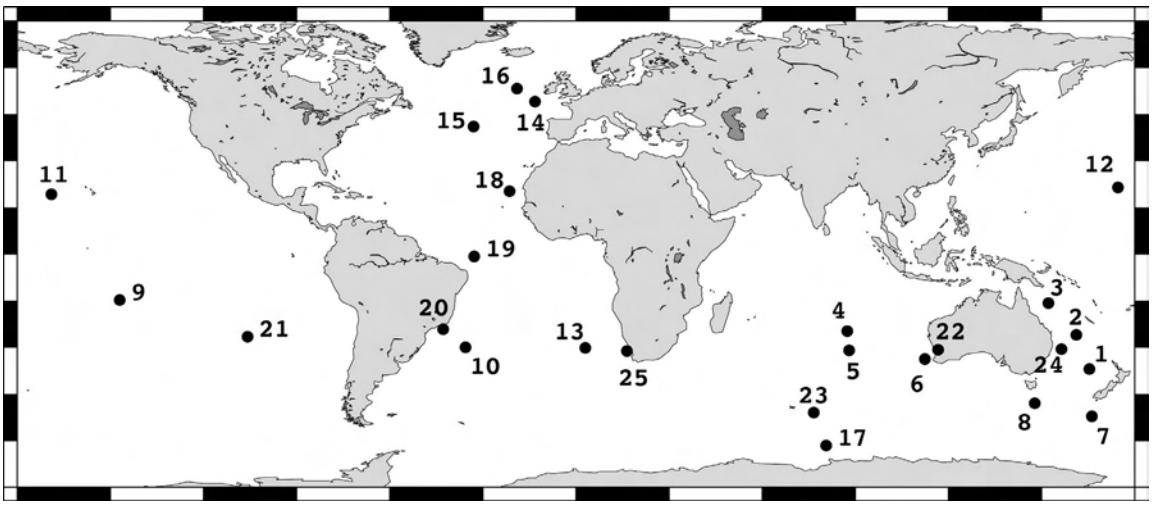

FIGURE 5—Map showing the location of fossil and modern samples included in the present study. See Appendix 2 for locality information corresponding to the numbers on the map. This map was created using the Online Map Creation web site (http://www.aquarius.geomar.de/omc_intro.html).

TABLE 5—OTU by character matrix. Polymorphic assignments are indicated by letters: a = 0&1, b = 1&2. OTUs are sorted alphabetically according to the species to which they are assigned, with described *Poseidonamicus* species listed first, followed by informal *Poseidonamicus* species and then outgroup OTUs. See Appendix 3 for a description of all characters and their states.

OTU name	Species assignment	Characters 1 2 3 4 12345678901234567890123456789012345678901234567890123456789012
ant-M1	*anteropunctatus*	100000?0000111010?0010b0?0100000000100001
ant-E1.2	*dinglei*	100000?0000111010000101000100000000001a0001
maj-H2	*major*	0000011000000211101010000110000000000010001
maj-P23.Q23	*major*	000001a000000211201010000110000000000010001
maj-Q4.5	*major*	0000011000000211101010000110000000000b0001
min-P2	*minor*	0000011?000002112010100011100001000 00b0001
min-Q1	*minor*	0000011?0?000211201010001110000100000b0001
mio-M1.3	*miocenicus*	00000100a11012011110100000a000000000010001
mio-M2.P12.PAG	*miocenicus*	00000100aa1012a11a10100000a000000000010001
mio-P3.5	*miocenicus*	0000010?a11012011110100000?000000000010001
mio-P4	*miocenicus*	0000010?a11012011110100000a000000000010001
nud-Q1.2	*nudus*	00000???000111?????01?420??00000?000100001
ocu-Q1.2	*ocularis*	0000011100000211 10?0100001?000000000011001
pan-H1	*panopsus*	101001??000010010??1?000?0000000000001000?
pin-H3	*pintoi*	0000010000001210111010000010000000000020001
pin-P1.2	*pintoi*	000001000000121011101000 0a10000000000b0001
pin-Q234	*pintoi*	0000010000001210 1a1010000010000000000010001
rio-P1	*pintoi*	000001a0a000121a2110100000000000000000010001
nud-M2	*praenudus*	00000???000111?a??001?4b00?00000?000100001
pse-O1	*pseudorobustus*	11110???00001b010?001000?000000000000a0101
pun-Q1	*punctatus*	000000??000111000??01?3000?000000000110001
rio-M1	*riograndensis*	0000011000001210 1?101000?0100001000010001
rio-M23	*riograndensis*	000001100000121a11101000001000101000010001
rio-M456	*riograndensis*	000001a000001210111010000001000a01000010001
rob-O1	*robustus*	111100??0??0110100?0100000010?00000010?01
rud-E1	*rudis*	111100?0000011010000100000010000000 0a0101
rud-O1	*rudis*	111100?0000011010000100000010000000000010001
rud-Q1.2	*rudis*	111100?000001a01aa00100000011100000000010001
spF-E1	species 1	??000110aa001ba11010100000100000000?10001
spE-O12	species 2	1000011100001211101010000010000000000a10?01
gr1-H1.2	species 3	0000011111a012a1a?10100000100000000000010001
gr3-H1.2	species 4	000001010a0012a11a10102000100000000000010001
gr3-P1.2	species 4	00000101010012a11010100000100000000000b0001
min-H1	species 5	0000011000000211 1a1010001110000000000a0001
min-M2	species 5	000001a000000211b01010001110000000000010001
spB-O1	species 5	000001a0000002111010100011100000000000010001
zAG-M1	*Agrenocythere hazelae*	101010??????10?1?1?021000?0?000000000010001
zBR-M1	*Bradleya dictyon*	20?0111?0?00100100?0010000 1000?00111010010
zBR-H1	*Bradleya normani*	????11??0??010010??0?100?01000?00111??001?
zHE-K1	*Hermanites sagitta*	10?01????0010010??1?100?00100??00000?0010

(London). Additional samples were provided courtesy of several deep-sea scientists. Some samples were collected by dredge, but most were from cores, largely from the Deep Sea Drilling Program (DSDP). Current published age models were available for several studied cores. For the remaining cores, age-depth models were created based on biostratigraphic occurrence data (mostly from the DSDP Initial Reports), updated to the most recent syntheses of Cenozoic chronostratigraphy (Berggren et al., 1995a, 1995b). These updated age models are available upon request.

Each of the over 3,000 specimens included in this study was digitally imaged in lateral view with scanning electron microscopy (SEM), using low-vacuum or environmental SEM mode on uncoated specimens. Figured specimens were deposited in the National Museum of Natural History (Washington, DC, accession numbers USNM 527078-USNM 527096) or the Natural History Museum (London, United Kingdom; accession numbers OS16002-OS16011).

Operational taxonomic units.—Operational taxonomic units (OTUs) were defined as spatio-temporally restricted morphological clusters of specimens. Initially, most OTUs consisted of individuals from a single core or dredge sample. In order to achieve useful sample sizes in cores with many closely spaced samples, multiple samples were often combined into the same OTU. These lumped OTUs generally spanned less than a few hundred thousand years, although more extensive lumping was necessary for rare species such as *P. punctatus*. These OTUs were then scored for all phylogenetic characters. After this initial coding, sets of OTUs with no fixed character differences were combined (see Smith, 1994), yielding a total of 36 *Poseidonamicus* OTUs to be analyzed.

Defining OTUs as spatio-temporally restricted morphological clusters, rather than simply using species as OTUs, obviates the need to judge which populations are members of the same species before characters are analyzed. One disadvantage of this strategy is that phylogenetic analysis of informal OTUs cannot be related easily to previous work. Although the correspondence of species as defined in the fossil record to actual evolving lineages may be questioned (Smith, 1994), at the very least, species are important units of analysis in ecological, environmental, and evolutionary studies. This disadvantage was overcome by relating the phylogenetic results to existing and informal species boundaries. In this way, species-level taxonomy is overlain on a population-level analysis.

Locality, age, and instar sampling are reported for each OTU in Appendix 1. Details about each locality are provided in Appendix 2. OTU names follow a specific format, with two parts separated by a dash. The first three letters correspond to the species to which the OTU was assigned prior to analysis (Table 1). This initial judgment was only a convenience and has no influence whatsoever on the analysis. OTUs that were not clearly assignable to an existing species were designated informally (e.g., 'spB,' 'gr3'). The second part of the OTU name indicates its age (E = Eocene, O = Oligocene, M = Miocene, P = Pliocene, Q = Quaternary [Pleistocene], H = Holocene). The numbers or letters

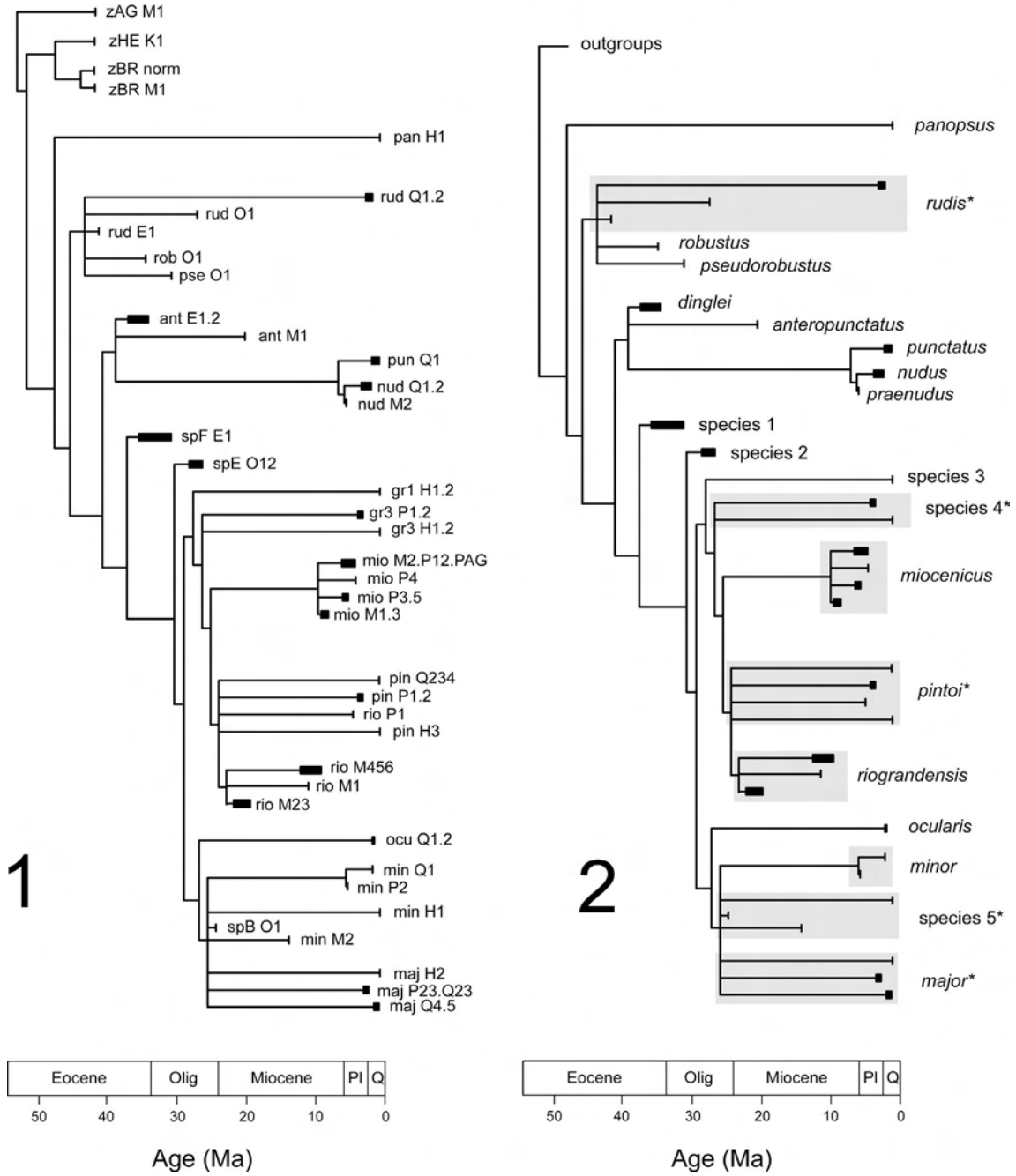

FIGURE 6—Phylogenetic results. *1,* Strict consensus of all equally parsimonious trees among OTUs. See Appendix 1 for information about each OTU. *2,* Same tree, but with OTU labels removed and OTUs assigned to existing or informal species. For both panels, OTUs are plotted according to their stratigraphic distribution, with the time scale shown on the bottom. Provisionally accepted metaspecies are indicated by an asterisk after their name (see text for details).

following the epoch code differentiate OTUs provisionally assigned to the same species and epoch. For example, the OTU rio-M1 includes specimens initially assigned to *P. riograndensis* from a single Miocene sample. Multiple letters and/or numbers indicate that more than one of the initial OTUs were combined because of compatible character coding (e.g., rio-M23 is comprised of individuals from two initially separate OTUs, rio-M2 and rio-M3). Outgroup OTU names were prefixed by the letter 'z' followed by the first two letters of its genus name, but otherwise followed the same naming conventions as ingroup OTUs.

All but one of the OTUs included in this study were examined using SEM. The one exception is OTU pan-H1, a representative of the shallow-water species *P. panopsus* Whatley and Dingle, 1989. This species has been reported only once in the published literature (Whatley and Dingle, 1989) and was not present in any of the collections examined. I was able to score this OTU for many characters from the numerous figures published with its description (Whatley and Dingle, 1989). Nevertheless, character data for this OTU was less complete than most other OTUs because of the lack of available material.

Jellinek and Swanson (2003) removed the species *P. ansoni* (Whatley et al., 1998) from *Poseidonamicus* and placed it in their new genus *Harleya*. I agree that this species does not belong in the genus *Poseidonamicus*, and thus have not included it in the present study. In addition to the morphological features described by Jellinek and Swanson (2003), *Harleya ansoni* differs from all

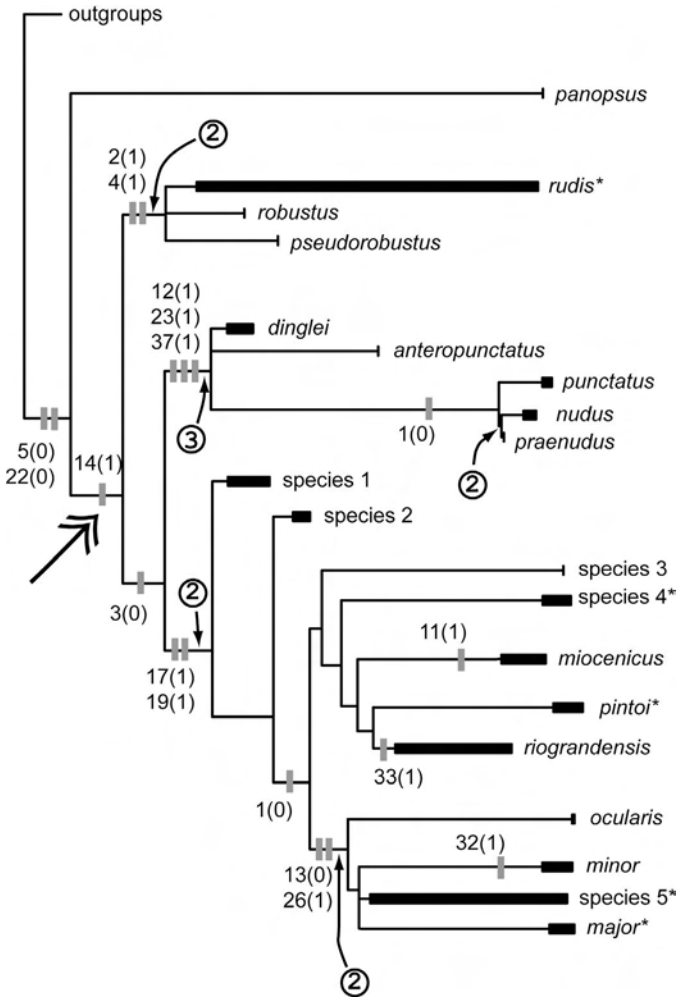

FIGURE 7—Condensed phylogenetic results. Same tree as in Figure 6, but with all species represented by a single branch. Hatchmarks indicate unambiguous synapomorphies with the character involved listed above or below the node and the derived state given in parentheses after the character number. Circled numbers indicate Bremer support; nodes without numbers have a Bremer support of one. As in Figure 6, metaspecies are indicated by an asterisk after their name. Large double-headed arrow indicates the sole transition from shallow to deep-sea habitat inferred by parsimony.

Poseidonamicus in at least three other features: 1) its much larger adductor muscle scar depression, 2) its polygonal rather than rounded anterior field fossae, and 3) its posterior region's distinctive shape in dorsal view (see characters 1, 22, and 42 in the phylogenetic analysis). In these features, *Harleya ansoni* is more similar to *Bradleya* than *Poseidonamicus*.

I studied the type material for 12 of the 15 described species of *Poseidonamicus* included in this study. The type material for *P. panopsus* was not personally examined because it is housed at the South African Museum, which I did not visit. In addition, type material for *P. miocenicus* Benson *in* Benson and Peypouquet, 1983 and *P. riograndensis*, while deposited at the Smithsonian Institution, could not be located in the collections of that museum. Nevertheless, these last two species are well represented in the current study, including ample material from their type locality (DSDP 526 on the Walvis Ridge of the South Atlantic Ocean).

Outgroups.—Four species from three genera were selected to be outgroups for phylogenetic analyses: *Bradleya dictyon* (Brady, 1880) (zBR-M1), *Bradleya normani* (Brady, 1865) (zBR-H1), *Hermanites sagitta* Bate, 1972 (zHE-K1), and *Agrenocythere hazelae* (van den Bold, 1946) (zAG-M1). These taxa were chosen because they are widely believed to be closely related to, but not descendants of *Poseidonamicus*. Benson (1972) placed *Bradleya* and *Poseidonamicus* into the same tribe, the Bradleyini, an opinion that was echoed in subsequent taxonomic works (Hartmann and Puri, 1974; Liebau, 1975). One of the *Bradleya* outgroups is the widespread deep-sea species, *B. dictyon* (zBR-M1, from a single sample from the late Miocene of DSDP 516). The other *Bradleya* outgroup is the species *B. normani* (zBR-H1, from several different modern localities, USNM catalogue numbers 174326, 174330, 174694, 188557, 190492). These particular species of *Bradleya* were chosen because their reticulation is similar in style to that of *Poseidonamicus*, simplifying morphological comparisons between these two genera.

Whatley and colleagues (Whatley et al., 1983; Whatley, 1985) suggested that *Hermanites sagitta* from the Late Cretaceous of Australia was closely related to the shallow-water ancestor of all *Poseidonamicus*. The OTU for *H. sagitta* (zHE-K1) is the type series for the species (NHM catalogue numbers IO4638-IO4642). The final outgroup is *Agrenocythere hazelae*, a species that is agreed to be more distantly related to *Poseidonamicus* than are the other outgroups (Benson, 1972; Hartmann and Puri, 1974; Liebau, 1975). This OTU (zAG-M1) includes individuals from a single sample from the Miocene of the South Atlantic (App. 1).

Characters.—A total of 42 characters with 53 derived character states were used to reconstruct the phylogeny of *Poseidonamicus*. Four of these were autapomorphies for individual OTUs, leaving 38 parsimony-informative characters. These characters captured variation in five aspects of the ostracode carapace: 1) internal morphology, 2) pores, 3) fossae arrangement, 4) muri, and 5) valve shape. All characters and their character states are described in Appendix 3, and the OTU by character data matrix is given in Table 5. In the following paragraphs, I will give a brief overview of each of the five character types. Readers are referred to Appendix 3 for details about individual characters including their defined states, how they were measured or scored, and reference to supporting figures.

The two internal carapace characters included in the present study involve the size and distinctness of the muscle scar depression (character 1), and the width of the calcified portion of the inner lamella (character 2). The relative paucity of internal carapace characters reflects the conservative nature of these features at low taxonomic levels (especially muscle scars and hingement, van Morkhoven, 1962). Although these features varied from specimen to specimen, the range of variability was nearly as broad within populations and species as it was across the entire genus, frustrating attempts to incorporate these characters into the analysis. Additionally, whereas it is easy to orient valves for external lateral view, internal morphology is more difficult to view from a consistent angle. As a result, subtle differences in morphology are more reliably observed in external than internal view.

Several previous studies have demonstrated that the presence/absence or location of homologous pores can be phylogenetically informative in ostracodes (Rosenfeld, 1982; Tsukagoshi, 1990; Hanai and Ikeya, 1991; Braccini et al., 1992; Kamiya and Hazel, 1992; Irizuki, 1993). Nine such characters are included in this study. One character involves the presence of murate pores between the anterior rim (AR) fossae (character 5). Two characters code for the number of pores along the anterior marginal rim peripheral to fossae AR1-AR6 (characters 3, 4). Two other characters concern the presence/absence of specific pores (characters 6, 8), and the remaining (characters 7, 9–11) describe variation in pore location.

Ten characters relate to the arrangement of fossae in the reticulum. One of these reflects the presence/absence of a fossa which appears to arise from division of the epidermal cell underlying the C3 fossa (character 12; see section on 'Ontogeny'). Another character reflects differences between *Poseidonamicus* and several of the outgroups with regards to the number of fossae bordering the AMR (character 21). The remaining eight characters

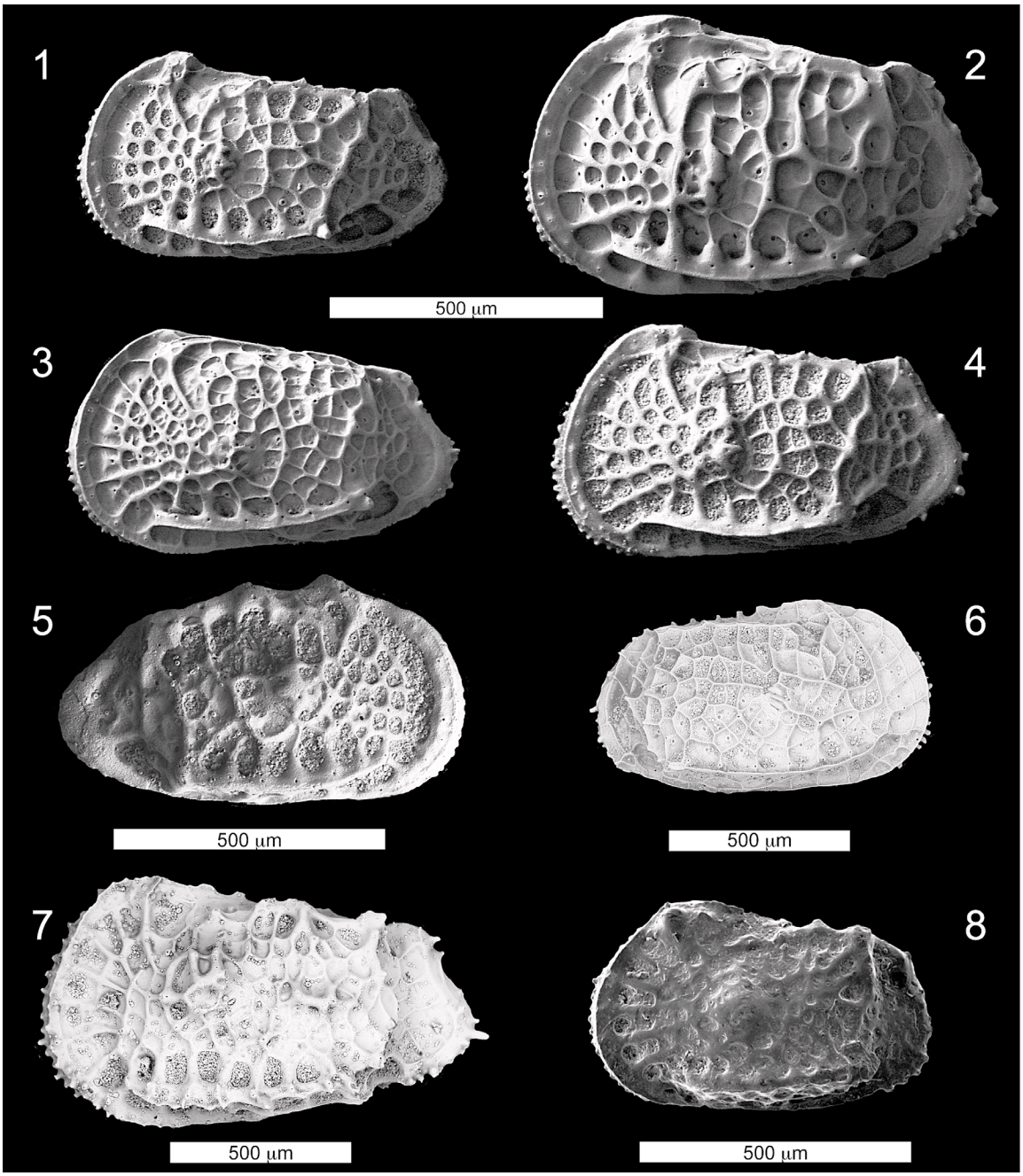

FIGURE 8—SEM images of *Poseidonamicus* species. *1–3*, *P. rudis* Whatley et al., 1986. *1,* Adult male LV from OTU rud-E1 (OS 16005). *2,* Adult female LV from OTU rud-Q1.2 (OS 16006). *3,* A-1 juvenile LV from OTU rud-Q1.2 (OS 16007). *4*, *P. pseudorobustus* Coles and Whatley, 1989, adult female? LV from OTU pse-O1 (OS 16004). *5*, *P. robustus* Whatley et al., 1986, adult male? RV from OTU rob-O1 (OS 16008). *6–8,* Outgroup taxa. *6*, *Bradleya dictyon* (Brady, 1880) from OTU zBR-M1, adult female RV (USNM 527078). *7*, *Agrenocythere hazelae* (van den Bold, 1946) from OTU zAG-M1, adult female LV (USNM 527079). *8*, *Hermanites sagitta* Bate, 1972 from OTU zHE-K1, adult female? LV (NHM type collection, IO4640). *1–4* share the same scale bar positioned in the middle of these four specimens.

capture variation in the shape (characters 18, 19) and relative position (characters 13–17, 20) of fossae in the reticulum, with a focus on those in the posterior field. Scoring several of these characters was problematic for *Poseidonamicus nudus* because fossae are difficult to discern in its much reduced reticulum. Similar difficulty was encountered in scoring these characters in *Agrenocythere hazelae*. Fossae arrangement in this species differs markedly from that in *Poseidonamicus*, complicating attempts to trace individual fossae between these genera. Characters for which relevant fossae were not clearly visible or of uncertain homology were coded as questionable (''?'') (Table 5).

Over a third of the characters in this study (15 of 42) describe aspects of the reticulum, including the occurrence and extent of secondary reticulation, details of the various ridges and spines, and the relative emphasis of some elements of the reticulum (characters 22–36). With one exception, these characters were defined to be independent of overall carapace robustness. The one exception is character 32, which reflects the robustness of juvenile

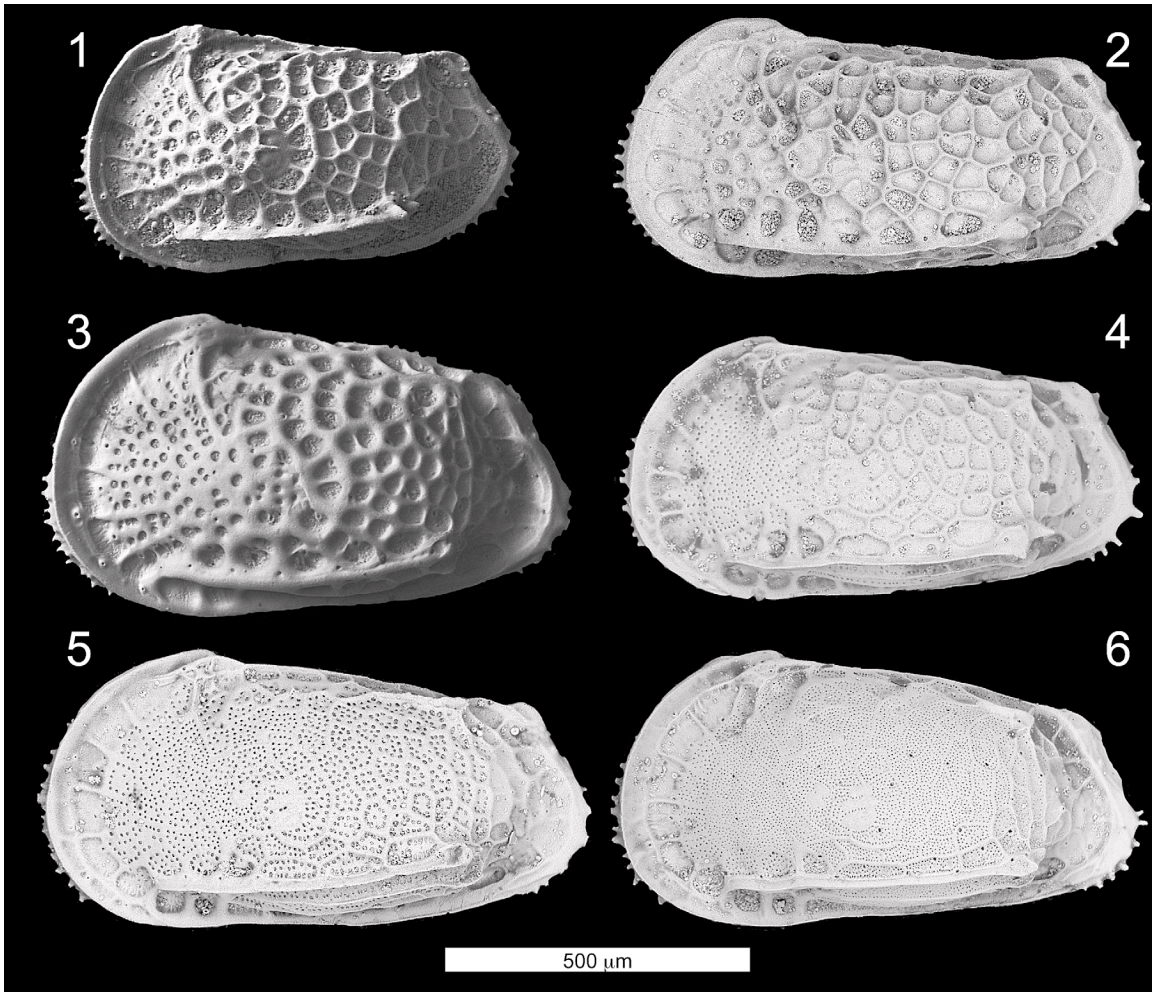

FIGURE 9—SEM images of *Poseidonamicus* species. *1*, *P. dinglei* Boomer, 1999, adult female LV from OTU ant-E1.2 (OS 16002). *2*, *P. anteropunctatus* Whatley et al., 1986, adult male LV from OTU ant-M1 (USNM 527080). *3*, *P. punctatus*, adult female? LV from OTU pun-Q1 (OS 16003). *4*, *P. praenudus* Whatley et al., 1986, adult male LV from OTU nud-M2 (USNM 527081). *5, 6, P. nudus* Benson, 1972. *5,* Adult male LV specimen not assigned to any OTU included in this analysis. This specimen is from the middle Miocene of DSDP 253 (253/7/4/110–116, 13.1 Ma, USNM 527082). *6,* Adult male? LV from OTU nud-Q1.2 (USNM 527083).

(A-1) individuals. Extreme robustness is a distinguishing feature of *Poseidonamicus minor*, and the muri of its penultimate instar are much coarser than those of all other species within the genus. Aside from this character, all others that refer to reticulum robustness consider thickness or extent of one mura relative to others nearby. As a result, these characters are unaffected by global increases or decreases in muri robustness which otherwise might induce dependence among characters.

Six characters describe aspects of overall carapace shape, including the relative elongation of the valves, the prominence of anterior cardinal angles, and the shape of the posterior portion of the valves in lateral and dorsal view (characters 37–42).

Although many species of *Poseidonamicus* are extant, the paucity of available specimens with preserved soft anatomy prevented the inclusion of any characters not observable from the calcified carapace (e.g., limbs). Samples from deep marine sediments very rarely contain live or recently dead ostracode specimens, presumably because of the very low population densities in this environment. Soft anatomy in *Poseidonamicus* has been described just once in the published literature (in Benson, 1972 for an undescribed species within this genus). Thus, while there is good reason to include characters based on soft anatomy whenever possible (Park et al., 2002), this approach is not currently feasible for *Poseidonamicus*.

Assumptions and methods.—There has been much debate among systematists as to the most appropriate procedure for translating morphological observations into coded characters for phylogenetic analysis. Three issues have been particularly controversial: the treatment of characters measured on a continuous scale, the coding of polymorphism, and the assumptions employed in the analysis of multistate characters. I will briefly describe my treatment of each of these issues.

I used a procedure similar to Swiderski et al. (1998) to divide continuously measured traits into discrete states. I created box plots for each character, and then determined cutoffs by eye that divided the distribution into relatively coherent groups. Although this approach is necessarily subjective, it allows for flexibility when measurement error varies with morphology (as was true for several characters in this study), or for those characters in which phenotypic variation differs greatly across OTUs (but see Wiens, 2001 for a discussion of some limitations of this approach).

Some characters were variable within OTUs. Of the various strategies available for coding variation within terminal taxa (Wiens, 1995, 2000), I used the common approach of treating multistate OTUs as polymorphic. Thus, when analyzed by PAUP*, polymorphic OTUs were reconstructed to have whichever state was more parsimonious in the context of the current tree. In order to reduce

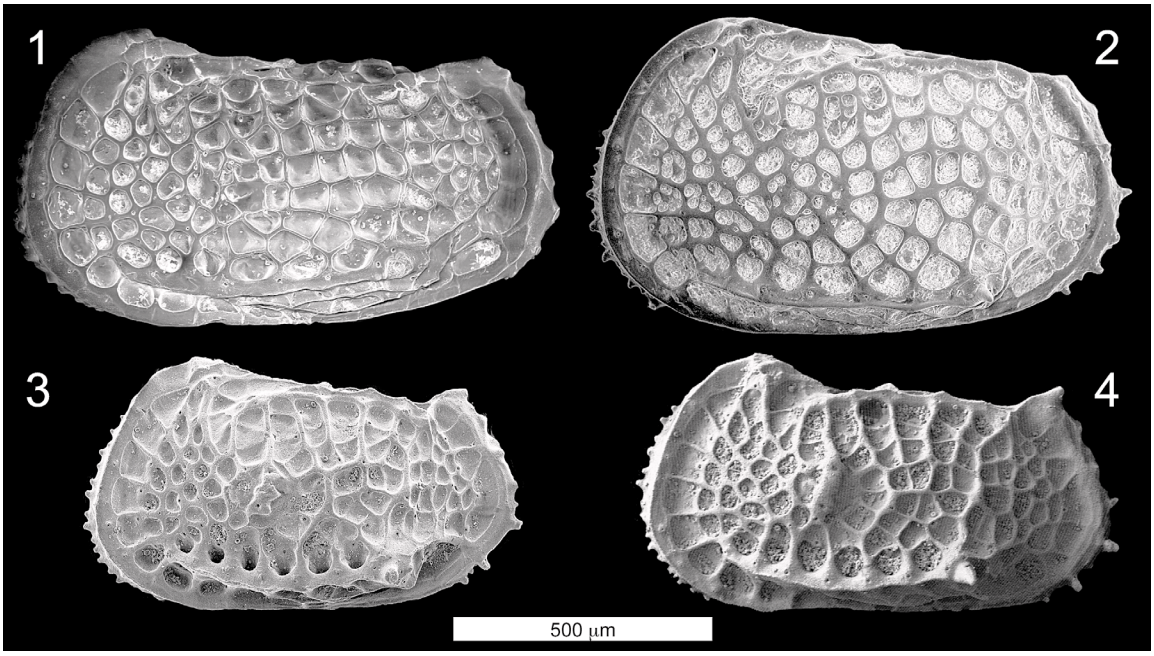

FIGURE *10*—SEM images of *Poseidonamicus* species. *1*, *P.* species 3, adult male LV from OTU gr1-H1.2 (USNM 527084). *2*, *P.* species 4, adult female LV from OTU gr3-H1.2 (USNM 527085). *3*, *P.* species 1, adult female LV from OTU spF-E1 (USNM 527086). *4*, *P.* species 2, adult male LV from OTU spE-O12 (OS 16009).

the noise arising from rare variants (the detection of which are heavily sample-size dependent, Swofford and Berlocher, 1987; Wiens, 1995), an OTU was coded as polymorphic only when at least 25% of its individuals displayed a variant character state. This use of a polymorphism threshold has been used occasionally (Mickevich and Johnson, 1976; Miyamoto, 1981; Good, 1988) in order to reserve polymorphic coding for instances of substantial within-population variation. Essentially, this approach is intermediate between what Wiens (1995) referred to as the ''polymorphic'' method (where any variation within an OTU results in a polymorphic code) and the ''majority'' method (where OTUs take the code of their most common character state).

In order to determine the sensitivity of the results to the method used to code characters variable within terminal taxa, I tried several alternate coding strategies. I first implemented methods that consider polymorphism an intermediate condition between fixed character state differences (using both the ''scaled'' and ''unscaled'' methods described by Wiens, 1995). Because coding methods that incorporate frequency information have performed well in several simulation and empirical studies (Wiens, 1995, 1998), I next implemented the frequency bins method of Wiens (1995). This approach was applied to all binary characters, with character weights chosen to equalize the contribution of polymorphic and non-polymorphic characters. Because frequency bins coding cannot be applied to multistate characters (which require more laborious and computationally intensive approaches, Wiens, 1999; Smith and Gutberlet, 2001), these characters were coded according to the 25% polymorphism threshold method as above (only one of the multistate characters included substantial polymorphism, so this omission should have little effect).

Thirty-five of the 42 characters included in this study have two defined character states. Among the seven multistate characters, six have three states and one has five states. For these multistate characters, it is necessary to specify the transition cost between each pair of states. Most commonly, this reduces to the question of whether characters should be treated as ordered or unordered (Hauser and Presch, 1991; Lipscomb, 1992; Wilkinson, 1992; Slowinski, 1993; Smith, 1994). Following Wilkinson (1992), Lipscomb (1992), and Slowinski (1993), among others, I ordered those multistate characters whose character states could logically be arrayed along a morphological gradient (see App. 3). Although there is some risk of assuming the wrong connectivity among character states, in my view this risk is outweighed by the gain in phylogenetic information when the assumed ordering is correct. Readers are referred to the above references for various perspectives on the merits and practice of ordering characters.

I used heuristic searching in PAUP* (Swofford, 2002) to find the optimal trees according to the maximum parsimony criterion. Branch swapping was done using the tree bisection reconnection option, and taxa were added by random sequence addition with at least 20 replicates. The strict consensus was used to summarize the resulting set of equally parsimonious trees, and Bremer support indices (Bremer, 1988) were calculated to evaluate character support for all nodes in the strict consensus.

Phylogenetic results.—The strict consensus of the 42,231 equally parsimonious trees is shown in Figure 6.1 with ingroup OTUs plotted according to their stratigraphic distribution (tree length = 122 steps, rescaled consistency index = 0.745). Despite the large number of equally parsimonious trees obtained, the strict consensus tree is reasonably well resolved, with most of the uncertainty near the tips of the tree (Fig. 6). The inclusion of multiple OTUs per species inflates the number of equally parsimonious trees because relationships among populations within a species are not usually resolvable. The Adams consensus tree (not shown) is very similar to the strict consensus, indicating that volatile OTUs are not unduly influencing the strict consensus tree.

Figure 6.2 shows the same strict consensus tree overlain with species-level taxonomy. OTUs were assigned to species on the basis of their correspondence to type material, published figures, and species descriptions. OTUs that could not be accommodated within existing species were assigned to informal numbered species. One or more OTUs were assigned to all valid species of *Poseidonamicus* (except for *P. whatleyi* Dingle, 2003) and to five informal species (species 1–5; Fig. 6.2). Five of these species (*P.*

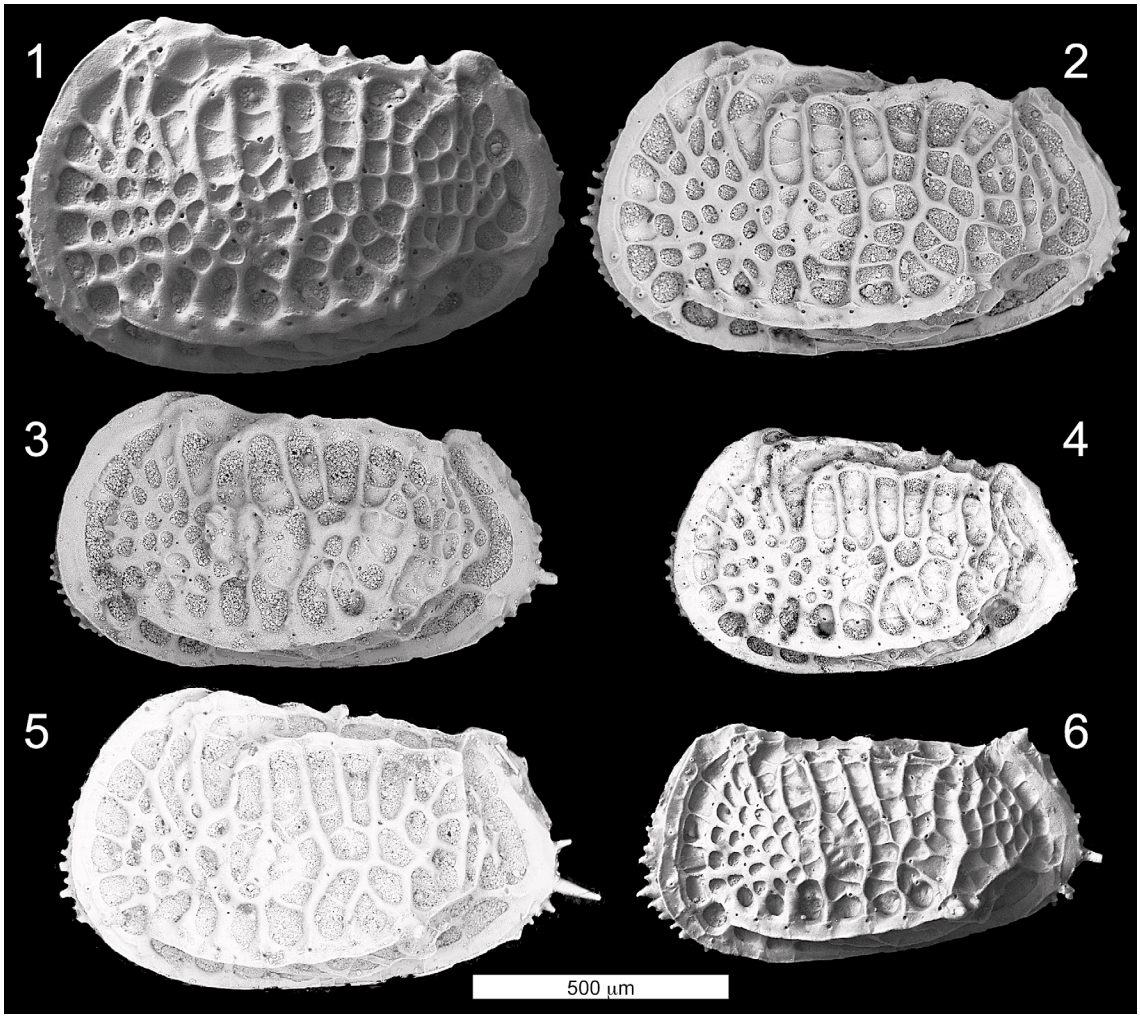

FIGURE *11*—SEM images of *Poseidonamicus* species. *1, 2*, *P. major* Benson, 1972. *1,* Adult female LV from OTU maj-Q4.5 (OS 16010). *2,* Adult male LV from OTU maj-H2 (USNM 527087). *3*, *P.* species 5, adult male LV from OTU min-M2 (USNM 527088). *4, 5*, *P. minor* Benson, 1972. *4,* A-1 juvenile LV from OTU min-Q1 (USNM 527089). *5,* Adult female LV from OTU min-Q1 (USNM 527090). *6*, *P. ocularis* Whatley et al., 1986, adult male LV from OTU ocu-Q1.2 (OS 16011).

rudis Whatley et al., 1986, *P. pintoi* Benson, 1972, *P. major* Benson, 1972, species 4, and species 5) are not demonstrably monophyletic; in some of the equally parsimonious trees they are true clades, but in others they are paraphyletic. These five species are therefore metaspecies (Donoghue, 1985), and are here provisionally accepted pending further evidence supporting or refuting their monophyly. I have followed the convention of labeling metaspecies with an asterisk to denote their uncertain status (Donoghue, 1985; Antsey and Pachut, 2004). In a separate work, I will evaluate the existing species of *Poseidonamicus* in light of this phylogenetic analysis and describe the informal species indicated in Figure 6.2. For the present study, however, I focus on the relationships among species of *Poseidonamicus* and the implications for morphological evolution in this group.

A simplified diagram of relationships among OTUs is presented to facilitate discussion of character evolution in *Poseidonamicus* (Fig. 7) showing all unambiguously reconstructed synapomorphies and Bremer support values for each node (circled numbers; nodes lacking numbers have Bremer support of one). This figure is simplified in that all OTUs assigned to the same species are represented as a single lineage, including the possibly paraphyletic metaspecies. It is important to note that all character reconstructions and Bremer support values were calculated using the original, complete phylogeny (Fig. 6.1). The condensed diagram (Fig. 7) is used only to simplify presentation of character evolution and OTU relationships. In the discussion that follows, readers are referred to Figures 6 and 7 for relationships among OTUs, Appendix 3 for character descriptions, and Figures 8–12 for SEM images of representative individuals from many of the OTUs. The stratigraphic ranges plotted in Figures 6 and 7 include only those OTUs in the present study, and thus must be underestimates of the true temporal span of these species. Even so, the information presented here extends the known ranges of several species. The ranges of *P. riograndensis* and *P. miocenicus* are extended forward in time to the Upper Miocene and Lower Pliocene, respectively, and the range of *P. dinglei* is extended backward to the Upper Eocene.

The phylogenetic results indicate that the genus *Poseidonamicus* is monophyletic with respect to the outgroup taxa. Two characters support *Poseidonamicus* as a clade: the absence of murate pores between the AR fossae (character 5), and the presence of distinctly rounded fossae and lower, broader muri in the anterior field of the reticulum (character 22). This latter feature is probably the easiest way to distinguish *Poseidonamicus* from similar genera and has long been considered characteristic of this genus (Benson,

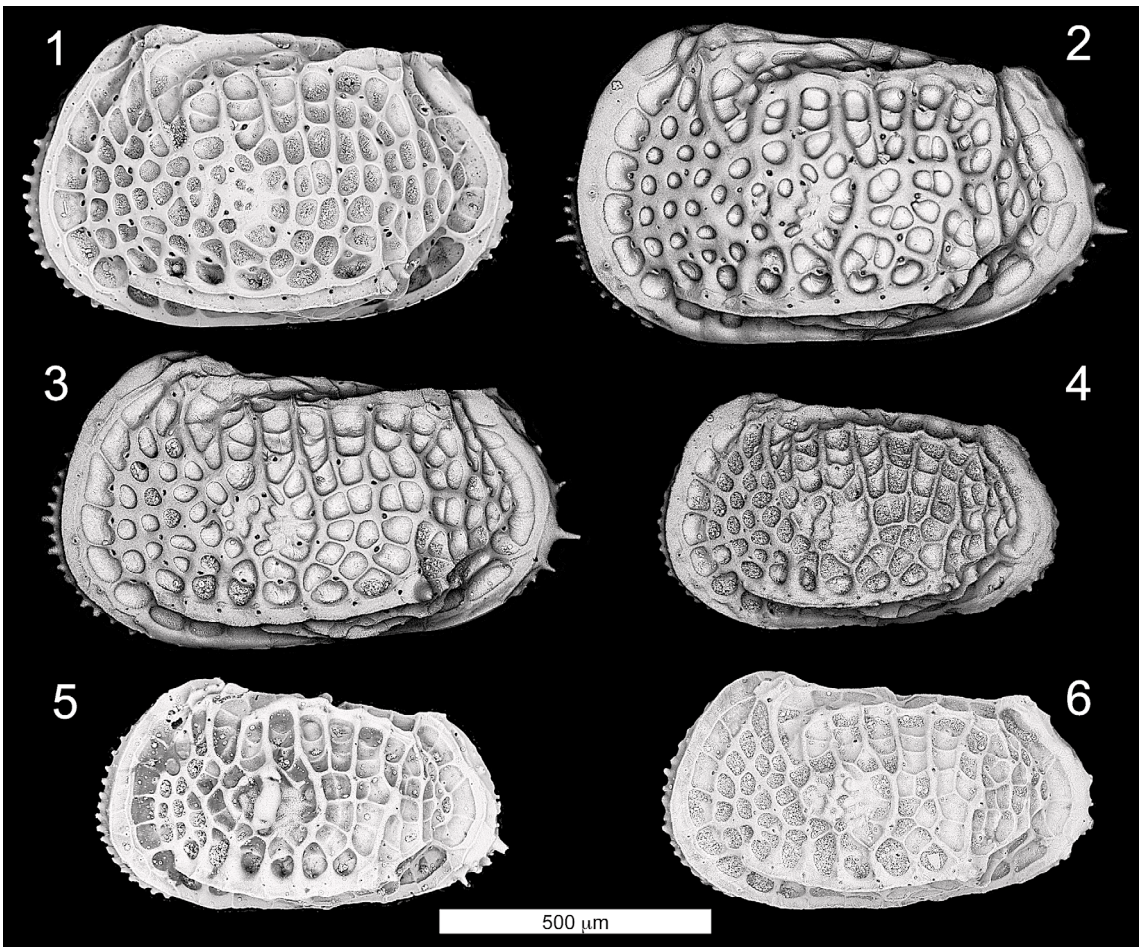

FIGURE *12*—SEM images of *Poseidonamicus* species. *1–3*, *P. pintoi*. *1,* Adult female LV from OTU pin-H3 (USNM 527091). *2,* Adult female LV from OTU pin-Q234 (USNM 527092). *3,* Adult male LV from OTU pin-Q234 (USNM 527093). *4*, *P. miocenicus* Benson *in* Benson and Peypouquet, 1983, adult male LV from OTU mio-M2.P12.PAG (USNM 527094). *5, 6*, *P. riograndensis*. *5,* Adult female LV from OTU rio-M23 (USNM 527095). *6,* Adult male? LV from OTU rio-M1 (USNM 527096).

1972; Whatley et al., 1986). All deep-sea species of *Poseidonamicus* also form a monophyletic group, with the shallow-water species *P. panopsus* basal to this large deep-sea clade. This clade is supported by one unambiguous synapomorphy based on the position of the A6 fossa (character 14), but this somewhat limited support may partly reflect uncertainty in scoring characters in *P. panopsus*. Further study of this species is necessary to clarify its character differences with deep-sea members of *Poseidonamicus*.

Among deep-sea *Poseidonamicus*, the clade comprised of *P. rudis*, *P. robustus* Whatley et al., 1986 and *P. pseudorobustus* Coles and Whatley, 1989 is sister to all other species. This clade, which has Bremer support of two, is supported by the presence of a relatively wide inner lamella (character 2), and the formation of an additional AMR pore during the molt between the A-1 and adult instars (character 4). Relationships among these three species are unresolved. This lack of resolution may be due in part to the paucity of material examined for *P. robustus* (only one adult, App. 1), which led to uncertain character state coding for this species (Table 5). Whereas *P. robustus* and *P. pseudorobustus* have rather restricted temporal distributions, *P. rudis* has the longest geological range within the genus, extending from the Eocene to the Quaternary. Although *P. rudis* has been described as morphologically static over this long interval (Whatley, 1985), Paleogene and Neogene representatives of this species differ in details of the DR (character 29), the morphology of the posterior denticles (characters 30), and in body size, with younger forms larger than older ones (this size difference is also documented by Ayress, 1994).

Sister to the *rudis–robustus–pseudorobustus* clade is a large group of species, all of which are characterized by the presence of five pores along the AMR in both the A-1 and adult instars (character 3). This large clade is divisible into two subclades. One is a well-supported group comprised of the species *P. dinglei*, *P. anteropunctatus*, *P. punctatus*, *P. praenudus*, and *P. nudus*, and the other includes all remaining deep-sea species.

The clade that includes *P. dinglei*, *P. anteropunctatus*, *P. punctatus*, *P. praenudus*, and *P. nudus* has strong character support. It has a Bremer support of three and unambiguous synapomorphies from three different types of characters. These synapomorphies include a divided C3 fossa (character 12), an inclined anterior marginal rim (character 37), and the presence in adults of at least some secondary reticulation in the anterior field (character 23). In the oldest and most robust member of this clade, *P. dinglei*, secondary reticulation is limited to the fossae immediately posterior to the AR fossae. Secondary reticulation is often more widespread in *P. anteropunctatus*, and it dominates the anterior field of *P. punctatus*, *P. praenudus*, and *P. nudus*. Finally, all members of this clade except for *P. punctatus* are rather elongate (character 38). Within this clade, the grouping of *P. punctatus*, *P. praenudus*, and *P. nudus* is supported by two features: an indistinct adductor muscle depression

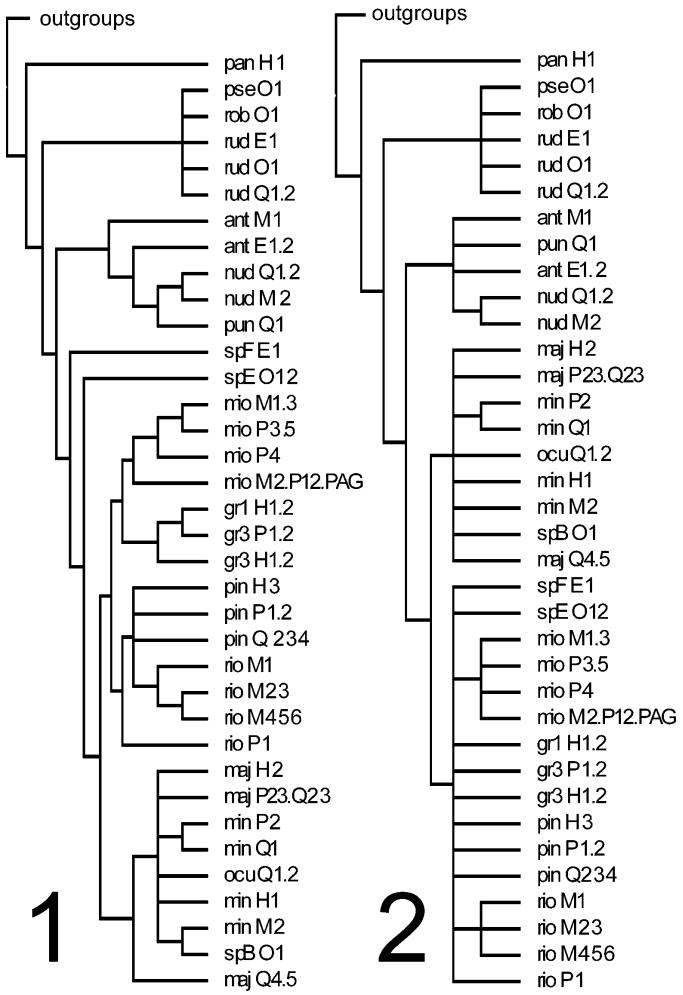

FIGURE *13*—Phylogenetic results using alternative character coding assumptions. *1,* Strict consensus of 40 equally parsimonious trees when polymorphic characters are coded using the frequency bins approach of Wiens (1995); see text for details. *2,* Strict consensus of 649,332 equally parsimonious trees when all characters are considered unordered.

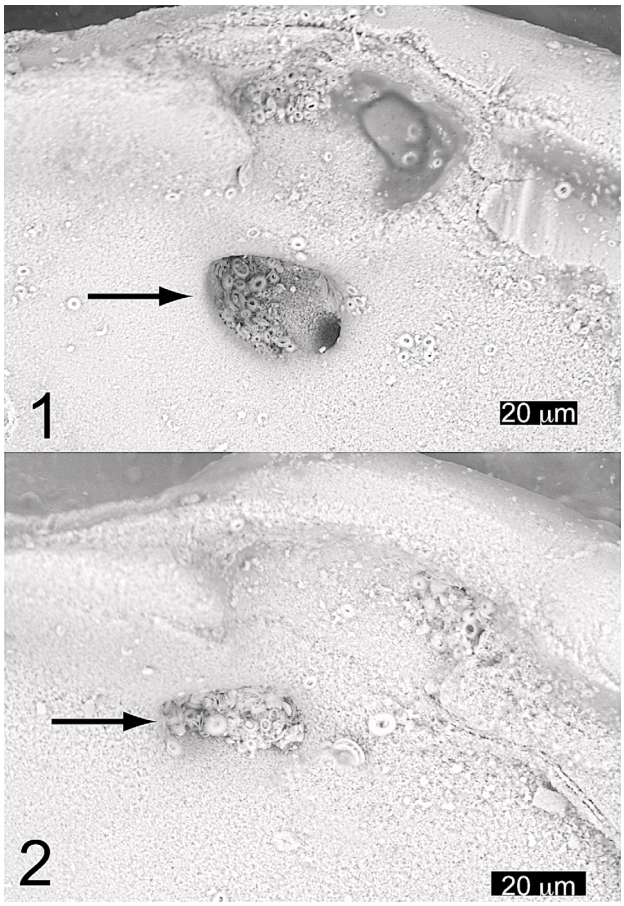

FIGURE *14*—Internal view of ocular region in A-1 juveniles. Arrows point to ocular sinus. *1*, *Poseidonamicus minor* from OTU min-Q1 (Quaternary, DSDP 208/2/4/50–56). *2*, *P. ocularis* from the same sample as *1* (OTU ocu-Q1.2).

(character 1), and dominance of secondary over primary reticulation in the anterior field (character 23).

The sister group to the *P. dinglei* through *P. nudus* clade includes all remaining OTUs in the analysis. OTUs in this group are characterized by the relatively posterior position of the C6 and D6 fossae (character 17) and the presence of a relatively wide AR7 fossa in the right valve of adults (character 19). Species 1 and then species 2 are sequential sister taxa to all remaining OTUs. These two informal species, despite a few character differences (Table 5), are morphologically quite similar (Fig. 10.3, 10.4).

Sister to species 2 is a clade characterized by a muscle scar depression that is indistinct anteriorly (character 1; this state is convergent with that of *P. punctatus*, *P. praenudus* and *P. nudus*). This clade is divided into one clade comprised of *P. major*, *P. minor*, *P. ocularis* Whatley et al., 1986, and species 5, and a second clade with *P. miocenicus*, *P. pintoi*, *P. riograndensis*, species 3 and species 4. The grouping of *P. ocularis* with *P. minor*, *P. major*, and species 5 is relatively well supported by the relative emphasis of muri in the posterior field (character 26) and the position of the A1 and B1 fossae (character 13). This latter character represents a relatively large change in fossae arrangement which gives the visual impression that the column of fossae posterior to the mural loop is ''double in the dorsal half, single in the ventral half'' (Ayress, quoted in Jellinek and Swanson, 2003). This arrangement is quite distinctive, allowing for nearly unambiguous allocation of specimens to this clade. However, it was sometimes difficult to assign OTUs to species within this clade, particularly for OTUs currently assigned to *P. major* and species 5. Whereas *P. ocularis* can be recognized by its distinctive anterior margin (character 39) and *P. minor* by its robust A-1 instar (character 32), differences between *P. major* and species 5 are more subtle. I have provisionally allocated OTUs with very shallow anterior field fossae as juveniles (character 25) to species 5, and those with more normally excavate fossae to *P. major*, but species groupings among these OTUs warrant further study.

The clade sister to the *major–minor–ocularis*–species 5 clade is comprised of OTUs almost entirely from the Atlantic Ocean and includes the species *P. miocenicus*, *P. pintoi*, *P. riograndensis*, species 3, and species 4 (Figs. 10.1, 10.2, 12). Despite its geographic coherence, neither the monophyly of this clade nor the relationships among its OTUs have very strong character support. Although synapomorphies unite OTUs within the species *P. miocenicus* and *P. riograndensis*, none unambiguously support this clade as a whole nor any relationships among its species.

The major features of this phylogenetic hypothesis (Fig. 6) are not very sensitive to particular assumptions about character coding. For example, the consensus tree resulting from frequency bin coding of polymorphic characters (Fig. 13.1) is almost completely consistent with the original consensus tree (Fig. 6), as are those resulting from application of the ''scaled'' and ''unscaled'' methods for coding polymorphism (not shown). In addition, the tree

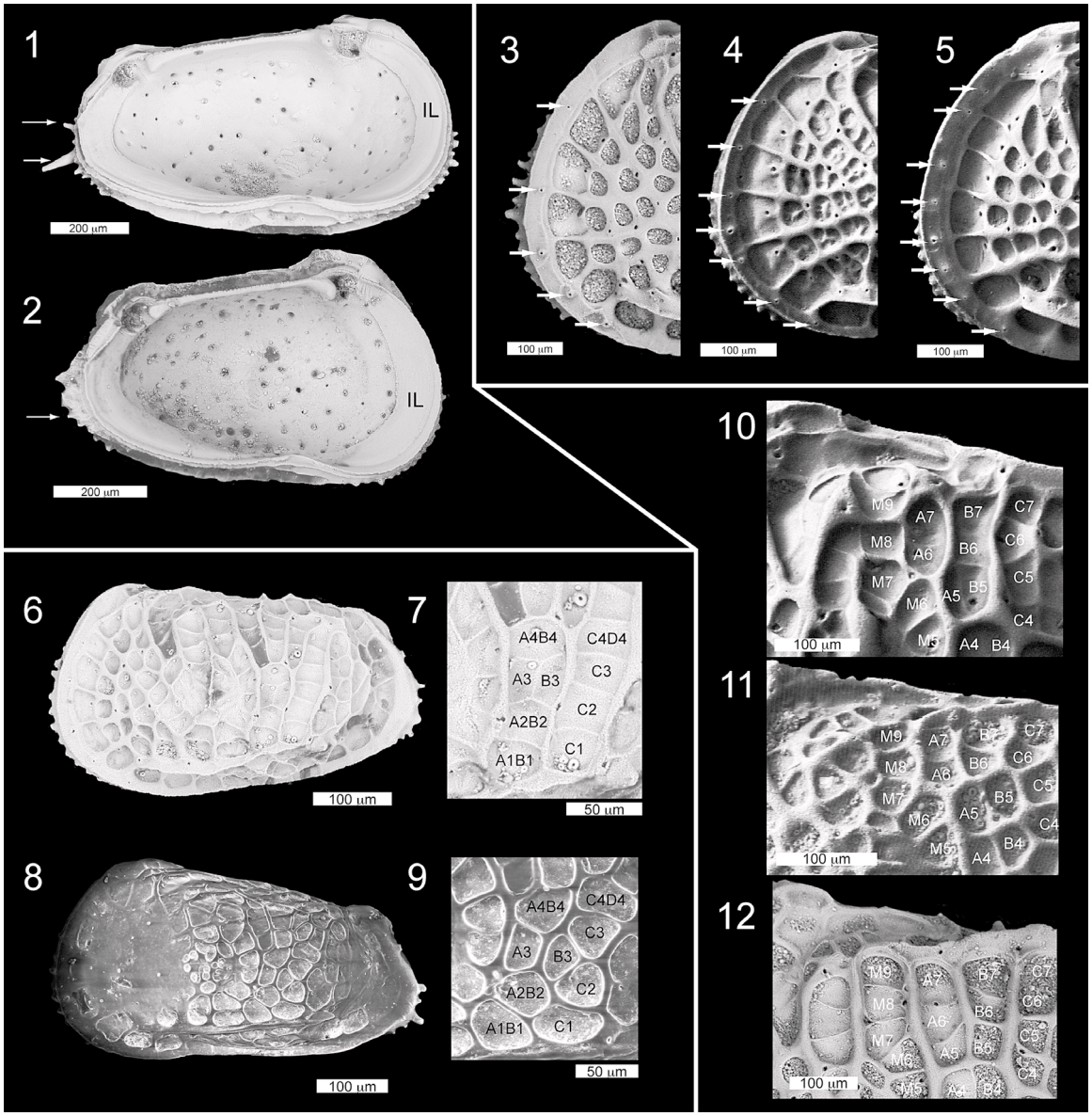

FIGURE *15*—Illustration of characters used in the phylogenetic analysis. *1, 2,* Characters 2 and 30, with arrows indicating posterior denticles. *1,* Specimen with a narrow IL (character 2, state 0) and unconnected denticles (character 30, state 0). *2,* Specimen with a broad IL (character 2, state 1) and fused denticles (character 30, state 1). *3–5,* Characters 3 and 4, with arrows indicating the presence of five (*3*), seven (*4*), and eight (*5*) AMR pores. *6–9,* A-2 specimens showing characters 18 and 25. *6,* Specimen with excavate anterior field fossae (character 25, state 0). *7,* Close-up of posterior field, showing subrectangular B3 fossa (character 18, state 1). *8,* Specimen with nearly smooth anterior field (character 25, state 1). *9,* Close-up of posterior field, showing triagonal B3 fossa (character 18, state 0). *10–12,* Character 14, showing specimens with A6 fossa located dorsal to M6 (*10*), dorsal to both M6 and A5 (*11*) and dorsal to A5 (*12*).

obtained by treating all characters as unordered (Fig. 13.2) is similar to the original consensus, albeit with some loss of resolution. Importantly, all nodes that are strongly supported in the original analysis (Bremer support > 1) are also recovered using these alternate assumptions, and the evolutionary scenarios discussed below hold equally well under these alternative topologies.

DISCUSSION

History of Poseidonamicus.—Although no formal cladistic analysis of this genus had been attempted previously, the findings of this study agree with several suggestions about relationships within the genus. For example, Whatley and Dingle (1989) suggested that the shelf-dwelling *P. panopsus* descended from the shallow water stock from which all deep-sea *Poseidonamicus* are derived. The basal phylogenetic position of this species in the current study supports this hypothesis. In addition, Whatley and colleagues (Whatley et al., 1983; Whatley, 1985) suggested that *P. rudis* and *P. robustus* were primitive among deep-sea *Poseidonamicus*, and most workers have recognized that *P. dinglei*, *P. anteropunctatus*, *P. punctatus*, *P. praenudus*, and *P. nudus* are closely related (Whatley et al., 1983; Boomer, 1999). Both of these notions are supported in the present study. Finally, a number of workers have suggested that *P. miocenicus*, *P. pintoi*, *P. riograndensis*, and *P. major* are relatively closely related (Benson and Peypouquet, 1983; Whatley et al., 1986; Steineck et al., 1988), a suggestion that, considered broadly, finds support in the analyses presented here.

Although many previous ideas about the phylogeny of *Poseidonamicus* find support in the present study, some do not. For example, Whatley and colleagues (Whatley et al., 1983; Whatley,

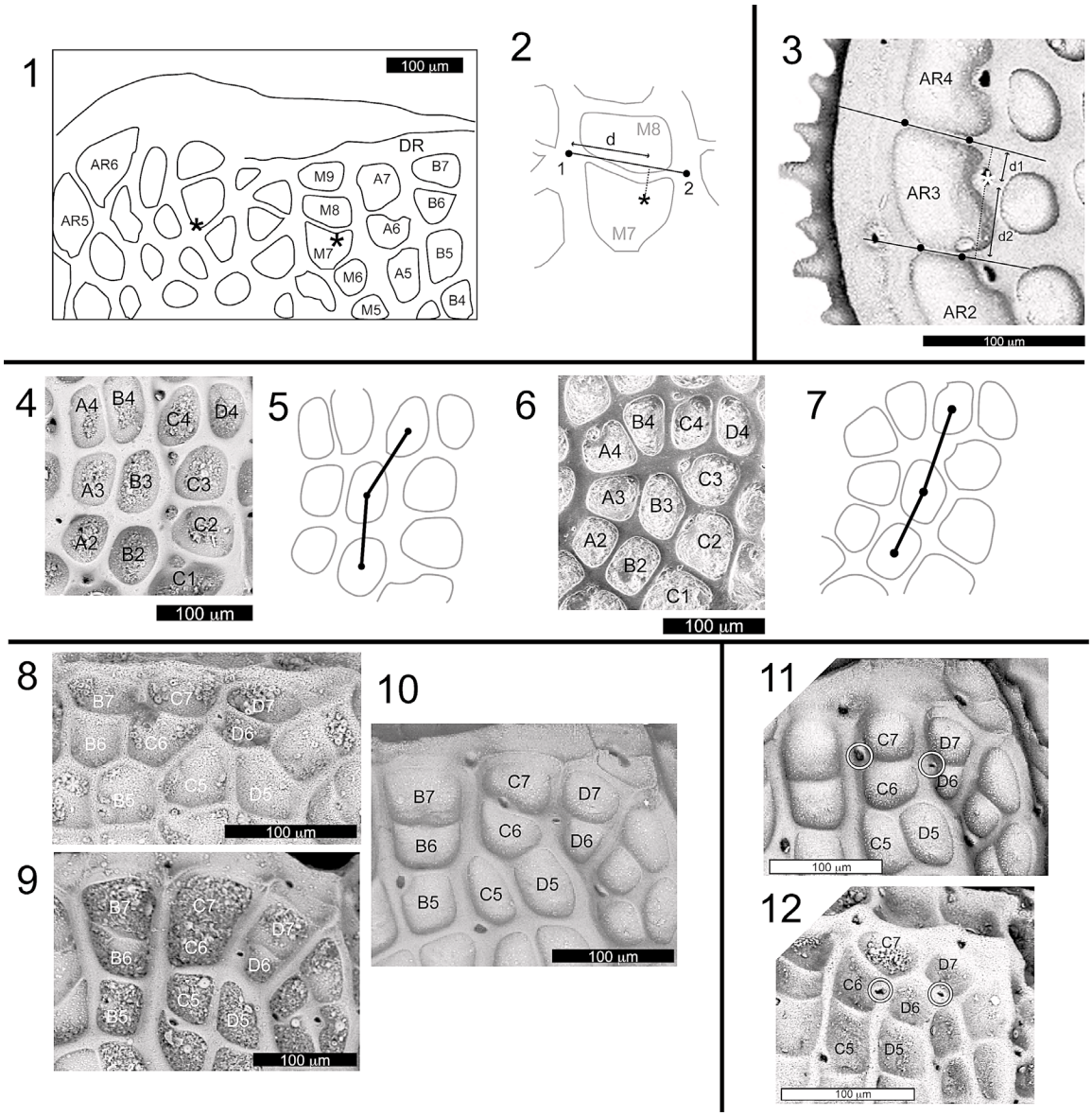

FIGURE *16*—Illustration of characters used in the phylogenetic analysis. *1, 2,* Characters 6–8. *1,* Line drawing with left most asterisk indicating the position of sieve pore of character 8, and rightmost asterisk indicating sieve pore of characters 6 and 7. *2,* Dimensions used to measure the position of this pore (character 7). *3,* Measurement of the dorsoventral position of the sieve pore in the AR3 fossa (character 9). *4–7,* Character 16. SEM image (*4*) and line drawing (*5*) of an individual with a relatively posterior C4 fossa (state 0). SEM image (*6*) and line drawing (*7*) of an individual with a relatively anterior C4 fossa (state 1). *8–10,* Character 17. Individuals with a C6D6 mura offset anteriorly (*8*), with no offset (*9*), and offset posteriorly (*10*), relative to the C5D5 mura. *11, 12,* Characters 10 and 11. *11,* Individual with an anteriorly located C67 sieve pore (character 10, state 0) and an anteriorly located D67 simple pore (character 11, state 0). *12,* Individual with a posteriorly located C67 sieve pore (character 10, state 1) and a posteriorly located D67 simple pore (character 11, state 1).

1985) postulated that *P. rudis* was directly ancestral to *P. minor* but these two species are only distantly related. Additionally, although Whatley et al. (1986) noted its resemblance to *P. major*, Whatley and Dingle (1989) suggested that *P. ocularis* was related to the shallow-water ancestors of *Poseidonamicus*. Such a basal position for this species is strongly contradicted in the present study, and the implications of this finding for the evolution of sightedness in *Poseidonamicus* are discussed below.

Phylogeny and the fossil record of Poseidonamicus.—The branching of taxa in a phylogenetic hypothesis makes testable predictions about the order of appearance of those taxa in the fossil record. Those clades relatively basal on the phylogeny should appear before clades that differentiated towards the tips of the tree. On the whole, phylogenetic relationships within *Poseidonamicus* are consistent with the order of appearance of clades in the fossil record. After the introduction of the genus to the deep sea, the most basal clade of *P. rudis*, *P. robustus*, and *P. pseudorobustus* appears first in the deep-sea fossil record (middle Eocene). The next clade towards the tips of the tree includes *P. dinglei* through *P. nudus*, whose first appearance is also early in the history of the genus (middle Eocene for *P. dinglei*). Tipward from this clade, we have species 1 and 2 from the late Eocene and Oligocene respectively, and beyond these is a large clade of mostly Neogene OTUs.

Although the deep-sea fossil record is generally in accord with the current phylogenetic results, at least one puzzling pattern remains. The shallow-water species *P. panopsus* is basal to all other species in the genus, but is known only from modern sediments. If its phylogenetic placement is correct, the lineage leading to

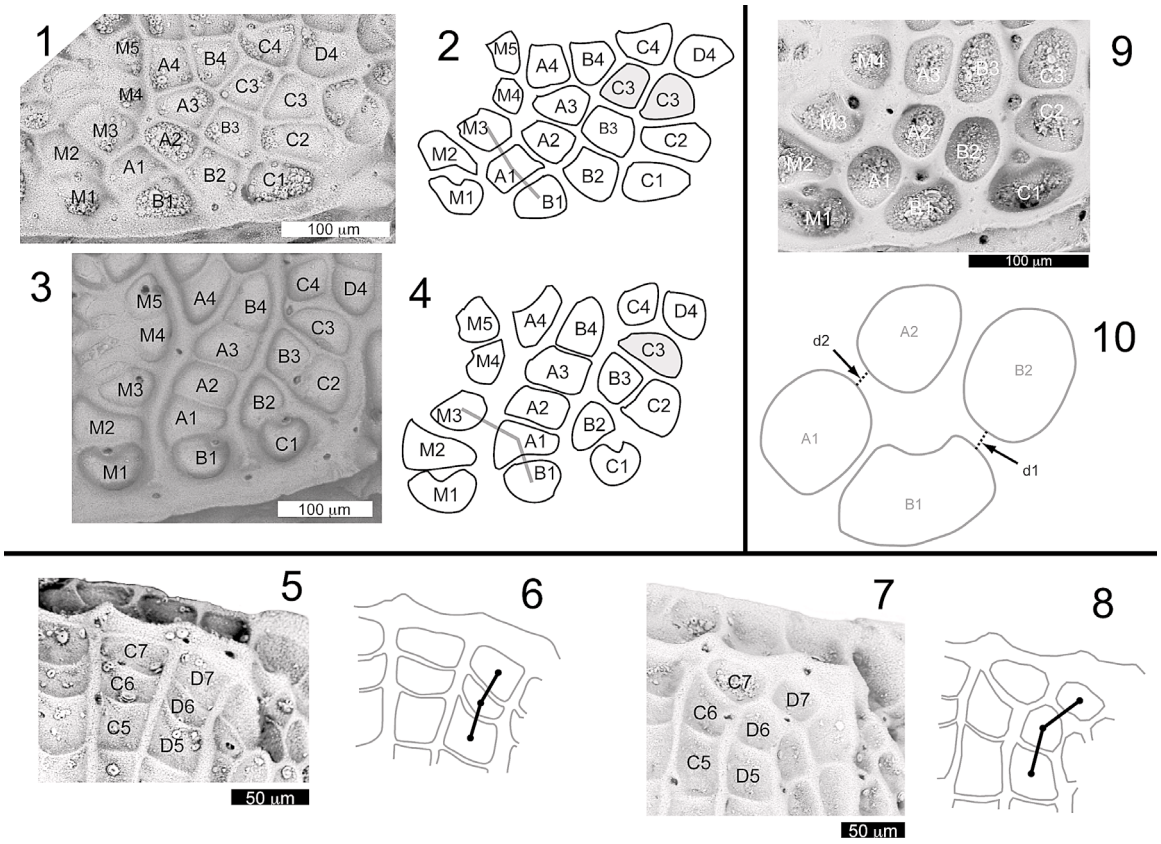

FIGURE *17*—Illustration of characters used in the phylogenetic analysis. *1–4,* Characters 12 and 13. SEM image (*1*) and line drawing (*2*) of an individual with a divided C3 fossa (character 12, state 1) and a B1 fossa located posteroventrally from fossa A1 (character 13, state 0). SEM image (*3*) and line drawing (*4*) of an individual with an undivided C3 fossa (character 12, state 0) and a B1 fossa nearly ventral to fossa A1 (character 13, state 1). Fossa C3 or its putative homologs are shaded grey. The grey lines indicate the angle measured for character 13. *5–8,* Character 15. SEM image (*5*) and line drawing (*6*) of an individual with an D7 fossa that is nearly dorsal, relative to D6. SEM image (*7*) and line drawing (*8*) of an individual with a more posteriorly located D7 fossa. *9, 10,* Character 26. SEM image (*9*) and line drawing (*10*) showing measurement of the thickness of the B1B2 mura relative to mura A1A2; the specimen shown has state (0).

modern *P. panopsus* has persisted from at least the middle Eocene to the present day without a known fossil record. One possible representative of this stock was described by Apostolescu (1961) as *Bradleya lagaghiroboensis* from the Paleocene of the Ivory Coast, later assigned to the genus *Quadracythere* Hornibrook, 1952 by Reyment (1963). Although the published photographs are quite small (Apostolescu,1961), the figured specimens appear similar to *Poseidonamicus* in overall shape, in the arrangement of muri in the reticulum, and in the presence of anterior field fossae that may be somewhat rounded. Clearly, it will be necessary to reexamine this material to evaluate the affinities of this taxon. It is possible that additional members of this lineage await discovery in the relatively understudied continental strata of western Africa.

Evolution of sightedness in Poseidonamicus.—The prominent eye tubercles and deep ocular sinuses of the shallow-water species *P. panopsus* and *P. whatleyi* indicate that they are capable of vision. All other species of *Poseidonamicus* lack these ocular features, live at great depth (>1 km), and are almost certainly blind. This difference between shallow- and deep-water forms indicates that there has been at least one evolutionary change in sightedness in this genus, the details of which have interested several previous workers. Two aspects of the evolution of sightedness have received particular attention: 1) the presence of putative ocular features in the deep-sea species *P. ocularis*, and 2) the suggestion that sightedness in shallow-water *Poseidonamicus* may be secondarily derived from blind ancestors (Dingle, 2003b). Both of these issues can be examined in light of the phylogenetic results of the present study.

In their comprehensive study of *Poseidonamicus* from deep-sea sediments in the southwest Pacific Ocean, Whatley et al. (1986) described the species *P. ocularis*. In their description they noted the presence of a small tubercle in the ocular region and a small but distinct ocular sinus, features they interpreted as rudimentary ocular structures. The reduced size of these structures, and the fact that this species was found only at depths greater than 1 km, led these authors to conclude that these structures were probably not functional. These authors suggested that although *P. ocularis* was likely blind, its ocular structures were vestiges of functional eyes in some relatively recent shallow-water ancestor. Whatley et al. (1986) predicted that further sampling of modern shallow marine sediments might find representatives of this of shallow-water ancestor of *P. ocularis*. At the time of this prediction, *Poseidonamicus* was known only from deep (>1 km) marine sediments. Nevertheless, this prediction was realized a few years later when Whatley and Dingle (1989) described the fully sighted species *P. panopsus* from continental shelf sediments off southwestern Africa.

Although the predicted discovery of shallow-water *Poseidonamicus* proved prescient, the evolutionary scenario upon which it was based is problematic because it implies that *P. ocularis* and *P. panopsus* should be closely related. The present phylogenetic analysis does not support this prediction—*P. ocularis* is closely

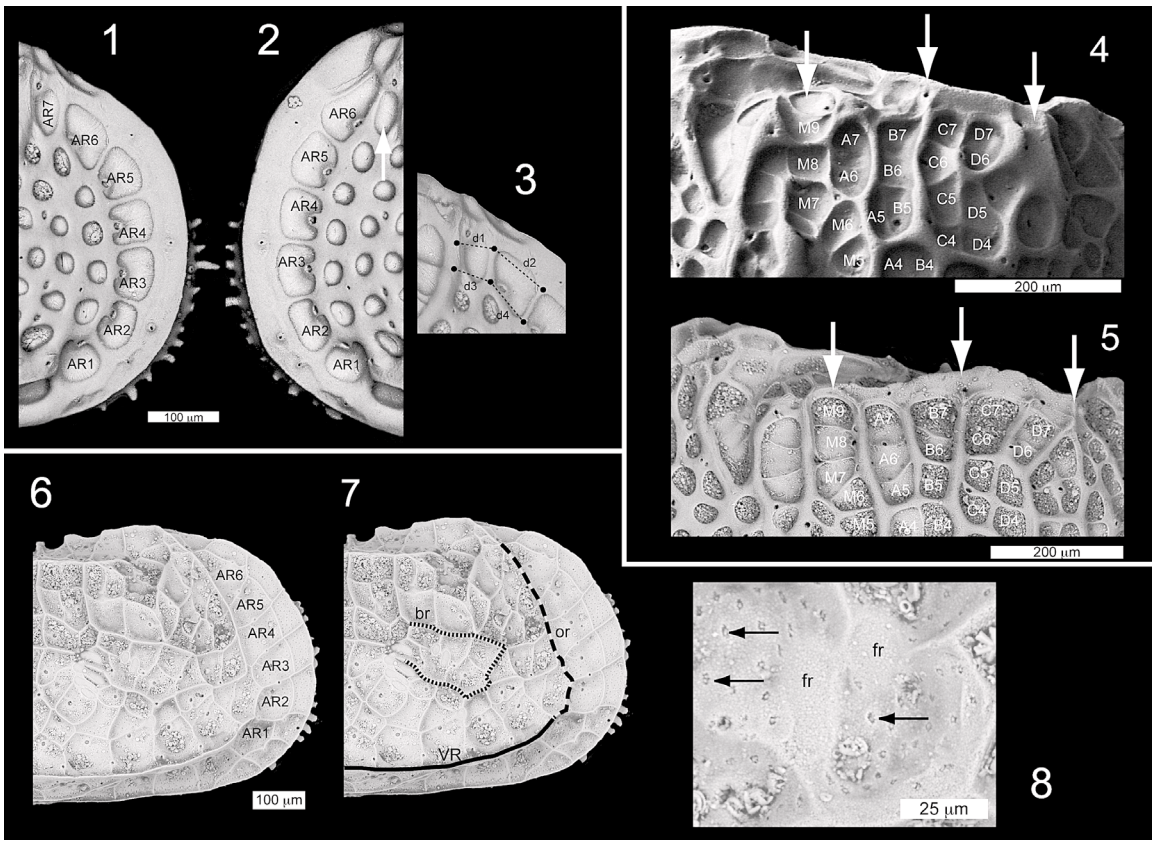

FIGURE *18*—Illustration of characters used in the phylogenetic analysis. *1, 2,* Character 21. AR fossae labeled in the RV (*1*) and LV (*2*) of *Poseidonamicus* Benson, 1972. There are six AR fossae in LV and seven in RV; the homolog of AR7 in RV is indicated with an arrow. *3,* Character 19, close-up of RV showing measurement of the width of the AR7 fossa. *4, 5,* Characters 27–29. *4,* SEM of an individual with a DR that is discontinuous above the mural loop (character 27, state 0), discontinuous just anterior to the C column of fossae (character 29, state 1) and terminates with a broad mura (character 28, state 1). *5,* SEM of an individual with a DR that is continuous above the mural loop (character 27, state 1), continuous above the C column of fossae (character 29, state 0), and terminates just posterior to fossa D7 (character 28, state 0). *6–8,* Characters 34–36. SEM image of RV adult *Bradleya dictyon* (zBR-M1) (*6*), with anatomical features indicated (*7*). or = ocular ridge, br = bridge, VR = ventrolateral ridge. *8,* Close-up of the area surrounding the frontal muscle scars of the same specimen as *6* and *7,* with arrows indicating individual foveola (character 36, state 1).

related to *P. major*, *P. minor*, and species 5 in a clade near the tips of the tree, whereas *P. panopsus* is located near the base of the tree, sister to all deep-sea *Poseidonamicus*. One cannot interpret these two species to be closely related without introducing a large amount of homoplasy; the shortest tree with *P. ocularis* and *P. panopsus* as sister taxa is eight steps longer than the most parsimonious trees. In an analysis of 38 parsimony informative characters, this is a very large difference. The fact that *P. ocularis* is nested deeply within a large clade of blind deep-sea taxa suggests that it evolved from blind ancestors. If so, this raises the question of how to account for its apparently ocular features.

There are at least three possible explanations for the putative ocular morphology of *P. ocularis*. First, it is possible that this species is truly closely related to *P. panopsus*, but has undergone massive convergent evolution with *P. major*, *P. minor*, and species 5. However, *P. ocularis* shares with these species a very characteristic arrangement of the A1 and B1 fossae (character 13), and many other features common to advanced members of this genus (Fig. 7). In fact, aside from its putative ocular structures, *P. ocularis* has no features that ally it with more basal members of the genus. The sheer number of convergences that would be required and the diversity of character systems that would need to be involved (pores, fossae, reticulum) argue very strongly that the advanced phylogenetic placement of *P. ocularis* is not the result of convergent evolution.

A second possibility is that a progenitor of *P. ocularis* migrated to shallower waters, reevolving eyes along the way. Then, *P. ocularis* reentered the deep sea, secondarily reducing its recently acquired ocular structures. This scenario is unlikely for several reasons. First, it requires the reevolution of complex structures, namely eyes, that have been lost. Although certainly not impossible (see below), this kind of evolutionary reversal is likely to be uncommon. Second, it postulates two large changes in habitat, from deep to shallow and back again, for which there is no direct evidence. Third, no shallow water forms similar to *P. ocularis* are known, but this is conceivably a failure of sampling.

A final possibility is that the ''ocular'' structures in *P. ocularis* have no relationship whatsoever to vision. Skeletal bumps and ridges in the ocular region are not uncommon among deep-sea *Poseidonamicus*, and it is possible that the putative ocular tubercle is a boss that is relatively large in this species for reasons unrelated to vision. This is the position of Mazzini (2005), who argues that the boss in the ocular region and its associated pore probably have a tactile sensory function. Indeed, while it is true that some individuals of *P. ocularis* have a relatively large boss in this region, some in fact do not (for example, Fig. 11.6). Moreover, the distinct ocular sinus of juveniles (Whatley et al., 1986) is actually a general feature of *Poseidonamicus*, and is not obviously more developed in *P. ocularis* than in related species such as *P. minor* (Fig. 14). However, three-dimensional casts of these sinuses (Kontrovitz and Yuhong, 1991) may be necessary to determine if the juvenile ocular sinus is subtly deeper or otherwise anomalous in

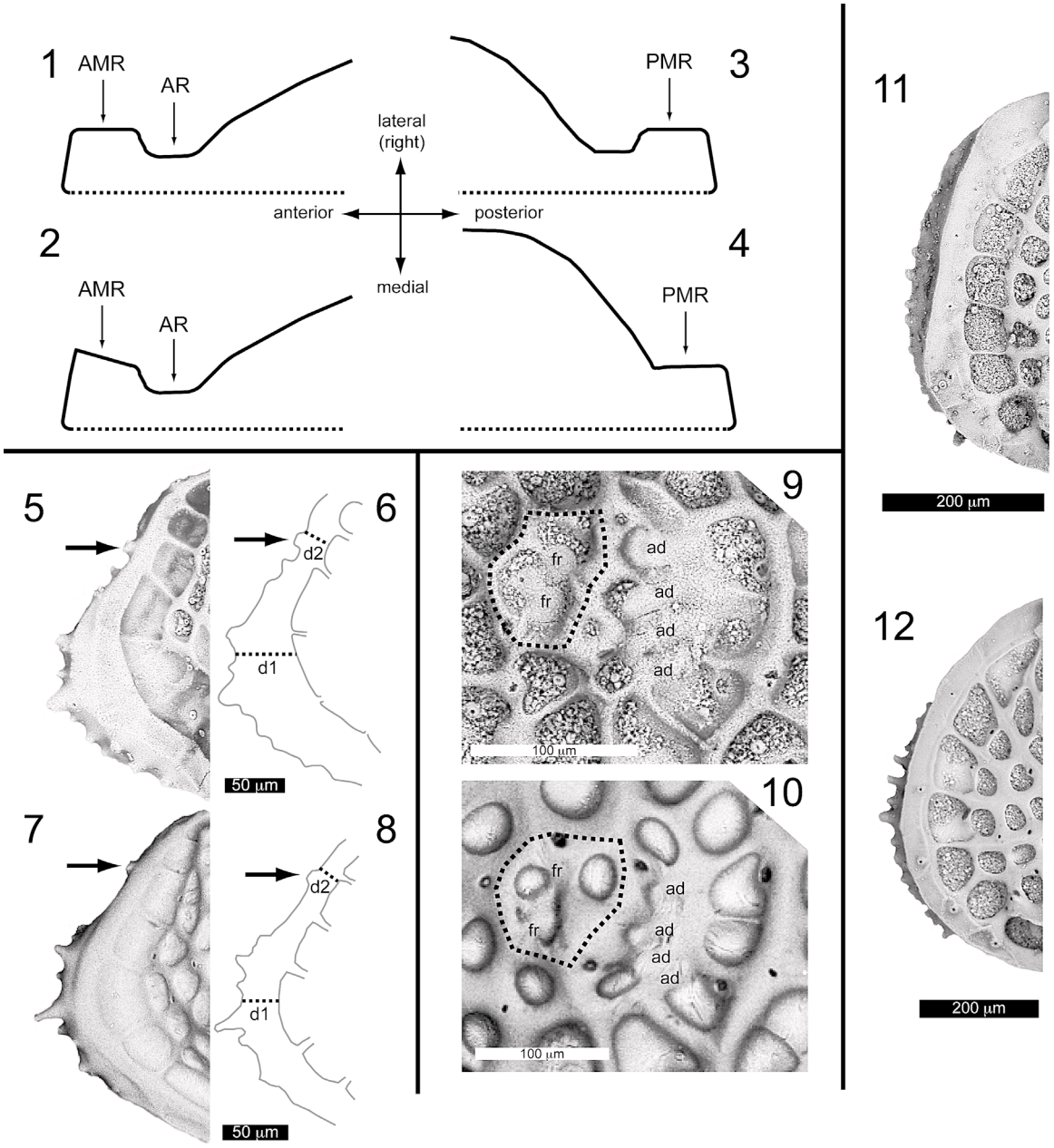

FIGURE *19*—Illustration of characters used in the phylogenetic analysis. *1, 2,* Character 37. Schematic drawing from dorsal view of the anterior portion of an RV, showing an individual with an flat (*1*) and upturned (*2*) anterior marginal rim. *3, 4,* Character 42. Schematic drawing from dorsal view of the posterior portion of a RV, showing an individual whose posterior region narrows immediately anterior to the PMR (*3*), and one whose posterior region increases in width immediately anterior to the PMR (*4*). *5–8,* Character 31. SEM image (*5*) and line drawing (*6*) of a specimen with a PMR expanded in width at the posterior extreme of the valve (state 1). SEM image (*7*) and line drawing (*8*) of a specimen with a PMR whose width is only moderately broader at the posterior extreme (state 0). The width d2 was measured immediately dorsal to a reference pore, which is indicated by an arrow. *9, 10,* Character 33. Close-up of the region including the adductor (ad) and frontal (fr) muscle scars, showing an individual with (*9*) and without (*10*) an open area in the reticulum near the frontal scars. Dotted lines delimit the open frontal area and its homologous region. *11, 12,* Character 39. SEM images of an individual with a 'squared off'(*11*) and more smoothly curving (*12*) anterior margin.

P. ocularis. Further evidence that the ocular sinus may not be preferentially developed in this species relative to its deep-sea congeners comes from Mazzini (2005), who reports that adult *P. ocularis* may lack an internal ocular sinus altogether.

In my view, the balance of evidence currently favors the third of these interpretations, which most parsimoniously explains the phylogenetic, morphological, and distribution data. If this analysis is correct, the predicted existence of shallow-water *Poseidonamicus* is remarkable in that it was based on an incorrect assumption, but nevertheless turned out to be true.

Although the deep-sea species *P. ocularis* may not have evolved directly from sighted ancestors, the genus *Poseidonamicus* does contain two species, *P. panopsus* and *P. whatleyi*, that are unambiguously fully sighted. Recently, Dingle (2002, 2003b) made the intriguing suggestion that these species may have evolved from blind ancestors, re-evolving eyes in apparent contradiction of Dollo's Law forbidding reevolution of complex features once they are lost (Gould and Robinson, 1994). Mathematical models of mutation accumulation suggest that such evolutionary reversals can be plausible over a few million years,

and potentially much longer if the genes involved are expressed in other developmental pathways (Marshall et al., 1994). Recent phylogenetic research supports the view that seemingly homologous complex structures can arise independently. For example, Oakley and Cunningham (2002) found that compound eyes in ostracodes originated independently from those in other crustaceans. In addition, there is now evidence for the independent acquisition of coiling in gastropods (Collin and Cipriani, 2003) and wings in insects (Whiting et al., 2003; but see the exchange between Trueman et al., 2004 and Whiting and Whiting, 2004). These findings suggest that Dollo's Law may not be as inviolable as once thought. As a consequence, the hypothesis that sighted *Poseidonamicus* species evolved from blind ancestors deserves careful consideration.

Dingle's hypothesis makes a clear and testable prediction: if phylogeny is reconstructed using traits unrelated to vision (as in the present study), *P. panopsus* and *P. whatleyi* should be most closely related to one or more blind members of the genus. While the phylogenetic position of *P. whatleyi* is unknown at present, the basal position of *P. panopsus* is inconsistent with the hypothesis that this species evolved from a blind deep-sea congener. Because *P. panopsus* is most parsimoniously inferred to be basal to the rest of *Poseidonamicus*, reconstructing sightedness in this species is strongly influenced by the primitive state of this feature in the outgroup genera. All *Hermanites* species are sighted, and although both *B. dictyon* and *B. normani* are blind, the genus *Bradleya* is primitively sighted (Whatley, 1985). While all species of *Agrenocythere* are blind, this is partly by definition because lack of eyes is a diagnostic feature of this genus (Benson, 1972). However, all taxa thought to be closely related to *Agrenocythere* Benson, 1972 are shallow-water forms (Benson, 1972; Liebau, 1975). These considerations suggest that the common ancestor of the outgroup OTUs is likely to have been a sighted, shallow-water species. Consequently, the most parsimonious reconstruction of sightedness in *Poseidonamicus* supports a single transition from sighted to blind in the lineage leading to the common ancestor of all known deep-sea species (Fig. 7). The loss of eyes in this lineage was presumably a consequence of the shift from a shallow to deep-sea habitat.

These phylogenetic considerations suggest that, contrary to Dingle's hypothesis, sightedness in *P. panopsus* is primitive rather than secondarily derived. However, it must be noted that this conclusion depends critically on the finding that *P. panopsus* is basal to the clade of deep-sea *Poseidonamicus*. Although this is the most parsimonious interpretation of the available character data, support for this particular aspect of the topology is not very deep (Bremer support is only one), and this conclusion should be considered accordingly provisional, pending further morphological and phylogenetic study of the sighted species assigned to this genus. Further resolution of the evolutionary relationships among these lineages should reveal whether eyes in *Poseidonamicus* provide yet another breach of Dollo's Law.

ACKNOWLEDGMENTS

I thank the members of my dissertation committee, M. Foote, D. Jablonski, M. LaBarbera, B. Chernoff, and T. Cronin for their advice, guidance, and comments on my thesis work and on an earlier version of this manuscript. I thank T. Cronin and R. Norris for generously providing deep-sea samples for study, and S. Schellenberg for allowing me to use his SEM images from ODP 744. Thanks also to G. Miller of the NHM, S. Whittaker at the NMNH, and A. Davis of the University of Chicago for help in SEM imaging. I am especially grateful to R. Benson and T. Cronin for their freely given time and knowledge on deep-sea ostracodes, and for welcoming me into this field. For discussion and suggestions, I thank K. R. Thomas, R. Lockwood, M. Kosnik, T. Rothfus, L. Park, M. Zelditch, and two anonymous reviewers; K. R. Thomas also provided much needed editorial help. This research was supported by student grants from Sigma Xi, The Hinds Fund of the University of Chicago, and The Paleontological Society and also by a Dissertation Improvement Grant from the National Science Foundation.

REFERENCES

ANTSEY, R. L., AND J. F. PACHUT. 2004. Cladistic and phenetic recognition of species in the Ordovician bryozoan genus *Peronopora*. Journal of Paleontology, 78(4):651–674.

APOSTOLESCU, V. 1961. Contribution a l'étude paléontologique (Ostracodes) et stratigraphique crétacés et tertiares de l'Afrique Occidentale. Revue de l'Institut Français de Pétrole et Annales des Combustibles Liquides, 16(7–8):779–867.

AYRESS, M. A. 1994. Cainozoic palaeoceanographic and subsidence history of the eastern margin of the Tasman Basin based on Ostracoda, p. 139–157. *In* G. J. van der Lingen, K. M. Swanson, and R. J. Muir (eds.), Evolution of the Tasman Sea Basin. A. A. Balkema Publishers, Rotterdam, Netherlands.

AYRESS, M. A., H. NEIL, V. PASSLOW, AND K. SWANSON. 1997. Benthonic ostracods and deep watermasses: A qualitative comparison of Southwest Pacific, Southern and Atlantic oceans. Palaeogeography, Palaeoclimatology, Palaeoecology, 131:287–302.

BATE, R. H. 1972. Upper Cretaceous Ostracoda from the Carnarvon Basin, western Australia. Special Papers in Palaeontology, 10, 148 p.

BENSON, R. H. 1972. The *Bradleya* problem, with descriptions of two new psychrospheric ostracode genera, *Agrenocythere* and *Poseidonamicus* (Ostracoda: Crustacea). Smithsonian Contributions to Paleobiology, 12, 138 p.

BENSON, R. H. 1983. Biomechanical stability and sudden change in the evolution of the deep-sea ostracode *Poseidonamicus*. Paleobiology, 9(4):398–413.

BENSON, R. H., AND J.-P. PEYPOUQUET. 1983. The upper and mid-bathyal Cenozoic ostracode faunas of the Rio Grande Rise found on Leg 72 Deep Sea Drilling Project. Initial Reports of the Deep Sea Drilling Project, 72: 805–818.

BERGGREN, W. A., F. J. HILGEN, C. G. LANGEREIS, D. V. KENT, J. D. OBRADOVICH, I. RAFFI, M. E. RAYMO, AND N. J. SHACKLETON. 1995a. Late Neogene chronology: New perspectives in high-resolution stratigraphy. Geological Society of America Bulletin, 107(11):1272–1287.

BERGGREN, W. A., D. V. KENT, C. C. I. SWISHER, AND M.-P. AUBREY. 1995b. A revised Cenozoic geochronology and chronostratigraphy, p. 129–212. *In* W. A. Berggren, D. V. Kent, M.-P. Aubrey, and J. Hardenbol (eds.), Geochronology, Time Scales and Global Stratigraphic Correlation. Vol. 54. Society for Sedimentary Geology, Tulsa, Oklahoma.

BOOMER, I. 1999. Late Cretaceous and Cainozoic bathyal Ostracoda from the Central Pacific (DSDP Site 463). Marine Micropaleontology, 37(2):131–147.

BRACCINI, E., J. P. PEYPOUQUET, AND R. H. BENSON. 1992. Quantization test of the evolution trend of Paleocosta pervinquieri (ostracode) during a 10-million period (Djebel-Dyr section, Paleogene, Algeria). Biosystems, 28: 153–167.

BRADY, G. S. 1865. On new or imperfectly known species of marine Ostracoda. Transactions of the Zoological Society of London, 5:359–393.

BRADY, G. S. 1880. Report on the Ostracoda dredged by the H.M.S. Challenger during the years 1873–1876. Reports of the Voyage of the H.M.S. Challenger, Zoology, 1, 184 p.

BREMER, K. 1988. The limits of amino-acid sequence data in angiosperm phylogenetic reconstruction. Evolution, 42(4):795–803.

CHAPLIN, J. A., J. E. HAVEL, AND P. D. N. HEBERT. 1994. Sex and ostracodes. Trends in Ecology and Evolution, 9(11):435–439.

COHEN, A. C., AND J. G. MORIN. 1990. Patterns of reproduction in ostracodes: A review. Journal of Crustacean Biology, 10(2):184–211.

COLES, G., AND R. C. WHATLEY. 1989. New Paleocene to Miocene genera and species of Ostracoda from DSDP sites in the North Atlantic. Revista Española de Micropaleontología, 21(1):81–124.

COLLIN, R., AND R. CIPRIANI. 2003. Dollo's law and the re-evolution of shell coiling. Proceedings of the Royal Society of London, series B, 270:2551–2555.

CRONIN, T. M., D. M. DEMARTINO, G. S. DWYER, AND J. RODRIGUEZ-LAZARO. 1999. Deep-sea ostracode species diversity: Response to late Quaternary climate change. Marine Micropaleontology, 37:231–249.

DINGLE, R. V. 2002. Insular endemism in Recent Southern Ocean benthic Ostracoda from Marion Island: Palaeozoogeographical and evolutionary implications. Revista Española de Micropaleontología, 34(2):215–233.

DINGLE, R. V. 2003a. Recent subantarctic benthic ostracod faunas from the Marion and Prince Edward Islands archipelago, Southern Ocean. Revista Española de Micropaleontología, 35(1):119–155.

DINGLE, R. V. 2003b. Some palaeontological implications of putative, long-term, gene reactivation. Journal of the Geological Society, London, 160: 815–818.

DONOGHUE, M. J. 1985. A critique of the biological species concept and recommendations for a phylogenetic alternative. Bryologist, 88(3):172–181.

GOOD, D. A. 1988. Phylogenetic relationships among Gerrhonotine lizards. An analysis of external morphology. University of California Publications in Zoology, 121, 139 p.

GOULD, S. J., AND B. A. ROBINSON. 1994. The promotion and prevention of

recoiling in a maximally snaillike vermetide gastropod—a case-study for the centenary of Dollo's Law. Paleobiology, 20(3):368–390.
HANAI, T., AND N. IKEYA. 1991. Two new genera from the Omma-Manganji ostracode fauna (Plio–Pleistocene) of Japan—With a discussion of theoretical versus purely descriptive ostracode nomenclature. Transactions and Proceedings of the Palaeontological Society of Japan, n.s. 163:861–878.
HARTMANN, G., AND H. S. PURI. 1974. Summary of neontological and paleontological classification of Ostracoda. Mitteilungen aus dem Hamburgischen Zoologischen Museum und Institut, 70:7–73.
HAUSER, D. L., AND W. PRESCH. 1991. The effect of ordered characters on phylogenetic reconstruction. Cladistics, 7:243–265.
HORNIBROOK, N. 1952. Tertiary and Recent marine Ostracoda of New Zealand. Palaeontological Bulletin of the New Zealand Geological Survey, 18: 5–82.
HUNT, G., AND R. E. CHAPMAN. 2001. Evaluating hypotheses of instar-groupings in arthropods: A maximum likelihood approach. Paleobiology, 27(3): 466–484.
IRIZUKI, T. 1993. Morphology and taxonomy of some Japanese hemicytherine Ostracoda with particular reference to ontogenetic changes of marginal pores. Transactions and Proceedings of the Palaeontological Society of Japan, n.s. 170:186–211.
IRIZUKI, T. 1994. Quantitative analysis of ontogenetic changes of cell-reflecting sculptures in Ostracoda (Crustacea). Journal of Paleontology, 68(5): 1067–1073.
IRIZUKI, T. 1996. Ontogenetic change in valve characters in three new species of *Baffinicythere* (Ostracoda, Crustacea) from northern Japan. Journal of Paleontology, 70(3):450–462.
JELLINEK, T., AND K. M. SWANSON. 2003. Report on the taxonomy, biogeography and phylogeny of mostly living benthic Ostracoda (Crustacea) from deep-sea samples (Intermediate Water depths) from the Challenger Plateau (Tasman Sea) and Campbell Plateau (Southern Ocean), New Zealand. Abhandlungen der Senckenbergischen Naturforschenden Gesellschaft, 558, 329 p.
KAMIYA, T., AND J. E. HAZEL. 1992. Shared versus derived characters in the pore-system of *Loxoconcha* (Ostracoda, Crustacea). Journal of Micropalaeontology, 11(2):159–166.
KONTROVITZ, M., AND Z. YUHONG. 1991. Stereoscopic study of the ocular sinuses of some Ostracoda. Revista Española de Micropaleontología, 23(1): 27–35.
LIEBAU, A. 1971. Homologous Sculpture Patterns in Trachyleberididae and Related Ostracodes. Nolit Publishing House, Belgrade, 93 p.
LIEBAU, A. 1975. Comment on suprageneric taxa of the Trachyleberididae s.n. (Ostracoda, Cytheracaea). Neues Jahrbuch für Geologie und Paläontologie Abhandlungen, 148(3):353–379.
LIEBAU, A. 1991. Skulptur-Evolution bei Ostrakoden am Beispiel europäischer ''Quadracytheren.'' Geologie und Paläontologie in Westfalen, 13:1–395.
LIPSCOMB, D. 1992. Parsimony, homology and the analysis of multistate characters. Cladistics, 8:45–65.
MADDOCKS, R. F. 1992. Ostracoda, p. 415–441. *In* F. W. Harrison and A. G. Humes (eds.), Crustacea.Vol. 9. Wiley-Liss, New York.
MARSHALL, C. R., E. C. RAFF, AND R. RAFF. 1994. Dollo's law and the death and resurrection of genes. Proceedings of the National Academy of Sciences USA, 91:12283–12287.
MAZZINI, I. 2005. Taxonomy, biogeography and ecology of Quaternary benthic Ostracoda (Crustacea) from circumpolar deep water of the Emerald Basin (Southern Ocean) and the S Tasman Rise (Tasman Sea). Senckenbergiana Maritima, 35(1):1–119.
MICKEVICH, M. F., AND M. S. JOHNSON. 1976. Congruence between morphological and allozyme data in evolutionary inference and character evolution. Systematic Zoology, 25:260–270.
MIYAMOTO, M. M. 1981. Congruence among character sets in phylogenetic studies of the frog genus *Leptodactylus*. Systematic Zoology, 30(3):281–290.
OAKLEY, T. H., AND C. W. CUNNINGHAM. 2002. Molecular phylogenetic evidence for the independent evolutionary origin of an arthropod compound eye. Proceedings of the National Academy of Sciences USA, 99(3):1426–1430.
OKADA, Y. 1981. Development of cell arrangement in ostracod carapaces. Paleobiology, 7(2):276–280.
OKADA, Y. 1982a. Structure and cuticle formation of the reticulated carapace of the ostracode *Bicornucythere bisanensis*. Lethaia, 15:85–101.
OKADA, Y. 1982b. Ultrastructure and pattern of the carapace of *Bicornucythere bisanensis* (Ostracoda, Crustacea), p. 229–267. *In* T. Hanai (ed.), Studies on Japanese Ostracoda. University of Tokyo Press, Tokyo.
OKUBO, I. 1975. *Callistocythere pumila* Hanai, 1957 and *Leguminocythereis bisanensis* sp. nov. in the Inland Sea, Japan (Ostracoda). Proceedings of the Japanese Society of Systematic Zoology, 11:23–31.
PARK, L. E., K. MARTENS, AND A. S. COHEN. 2002. Phylogenetic relationships of *Gomphocythere* (Ostracoda) in Lake Tanganyika, East Africa. Journal of Crustacean Biology, 22(1):15–27.
REYMENT, R. A. 1963. Studies on Nigerian Upper Cretaceous and Lower Tertiary Ostracoda, Pt. 2, Danian, Paleocene, and Eocene Ostracoda. Stockholm Contributions in Geology, 10:1–287.
ROSENFELD, A. 1982. Distribution patterns and development of sieve-pores in two Recent ostracode species. Micropaleontology, 28(4):372–380.
SLOWINSKI, J. B. 1993. ''Unordered'' versus ''ordered'' characters. Systematic Biology, 42(2):155–165.
SMITH, A. 1994. Systematics and the Fossil Record. Blackwell Scientific, Oxford, 223 p.
SMITH, E. N., AND R. L. GUTBERLET. 2001. Generalized frequency coding: A method of preparing polymorphic multistate characters for phylogenetic analysis. Systematic Biology, 50:156–169.
STEINECK, P. L., D. DEHLER, E. M. HOOSE, AND D. MCCALLA. 1988. Oligocene to Quaternary ostracods of the central equatorial Pacific (Leg 85, DSDP-IPOD), p. 597–618. *In* T. Hanai, N. Ikeya, and K. Ishizaki (eds.), Evolutionary Biology of Ostracoda. Elsevier, Kodansha, Japan.
SWIDERSKI, D. L., M. L. ZELDITCH, AND W. L. FINK. 1998. Why morphometrics is not special: Coding quantitative data for phylogenetic analysis. Systematic Biology, 47(3):508–519.
SWOFFORD, D. L. 2002. PAUP*. Phylogenetic analysis using parsimony (*and other methods). Sinauer Associates, Sunderland, Massachusetts.
SWOFFORD, D. L., AND S. H. BERLOCHER. 1987. Inferring evolutionary trees from gene frequency data under the principle of maximum parsimony. Systematic Zoology, 36:293–325.
SYLVESTER-BRADLEY, P. C., AND R. BENSON. 1971. Terminology for surface features in ornate ostracodes. Lethaia, 4:249–286.
TRUEMAN, J. W. H., B. E. PFEIL, S. A. KELCHNER, AND D. K. YEATES. 2004. Did stick insects *really* regain their wings? Systematic Entomology, 29: 138–139.
TSUKAGOSHI, A. 1990. Ontogenetic change of distributional patterns of pore systems in *Cythere* species and its phylogenetic significance. Lethaia, 23: 225–241.
VAN DEN BOLD, W. A. 1946. Contributions to the Study of Ostracoda with Special Reference to the Tertiary and Cretaceous of the Caribbean Region. J. H. deBussy, Amsterdam, 167 p.
VAN MORKHOVEN, F. P. C. M. 1962. Post-Paleozoic Ostracoda. Vol. 1. Elsevier, Amsterdam, 204 p.
WHATLEY, R. C. 1985. Evolution of the ostracods *Bradleya* and *Poseidonamicus* in the deep-sea Cainozoic of the south-west Pacific. Special Papers in Palaeontology, 33:103–116.
WHATLEY, R. C., AND R. V. DINGLE. 1989. First record of an extant, sighted, shallow-water species of the genus *Poseidonamicus* Benson (Ostracoda) from the continental margin of south-western Africa. Annals of the South African Museum, 98(11):437–457.
WHATLEY, R. C., S. E. DOWNING, K. KESLER, AND C. J. HARLOW. 1986. The ostracode genus *Poseidonamicus* from the Cainozoic of the D.S.D.P. sites in the S.W. Pacific. Revista Española de Micropaleontología, 18(3):387–400.
WHATLEY, R. C., C. J. HARLOW, S. E. DOWNING, AND K. J. KESLER. 1983. Observations on the origin, evolution, dispersion and ecology of the genera *Poseidonamicus* (Benson) and *Bradleya* (Hornibrook), p. 492–509. *In* R. F. Maddocks (ed.), Applications of Ostracoda. Department of Geosciences, University of Houston.
WHATLEY, R. C., A. MOGUILEVSKY, M. I. F. RAMOS, AND D. J. COXILL. 1998. Recent deep and shallow water Ostracoda from the Antarctic Peninsula and the Scotia Sea. Revista Española de Micropaleontología, 30(3): 111–135.
WHITING, M. F., AND A. S. WHITING. 2004. Is wing recurrence *really* impossible?: A reply to Trueman et al. Systematic Entomology, 29:140–141.
WHITING, M. F., S. BRADLER, AND T. MAXWELL. 2003. Loss and recovery of wings in stick insects. Nature, 421(6920):264–267.
WIENS, J. J. 1995. Polymorphic characters in phylogenetic systematics. Systematic Biology, 44(4):482–500.
WIENS, J. J. 1998. Testing phylogenetic methods with tree congruence: Phylogenetic analysis of polymorphic characters in phrynosomatid lizards. Systematic Biology, 47(3):427–444.
WIENS, J. J. 1999. Polymorphism in systematics and comparative biology. Annual Review of Ecology and Systematics, 30:327–362.
WIENS, J. J. 2000. Coding morphological variation within species and higher taxa for phylogenetic analysis, p. 115–145. *In* J. J. Wiens (ed.), Phylogenetic Analysis of Morphological Data. Smithsonian Institution Press, Washington, DC.
WIENS, J. J. 2001. Character analysis in morphological phylogenetics: Problems and solutions. Systematic Biology, 50(5):689–699.
WILKINSON, M. 1992. Ordered versus unordered characters. Cladistics, 8(4): 375–385.

ACCEPTED 9 DECEMBER 2005

APPENDIX 1—Summary information for OTUs. The first column lists the label assigned to each OTU before analysis and the second lists the species to which each OTU was assigned based on the phylogenetic results (see text for details). *N* indicates the number of specimens examined for each OTU, divided by instar (listed in order from adults to A-4, with each instar separated by a dash). Locality information is given in Appendix 2 and mapped in Figure 5. Core samples are specified by standard DSDP/ODP notation (core/section/interval, only giving the lower value for the interval range). If individuals for an OTU span more than two samples, the range of core samples are given, followed by the total number of samples included in parentheses. Ages are in millions of years before present.

OTU	Species	*N*	Locality	Samples	Age
ant-M1	*anteropunctatus*	15-2-0-0-0	DSDP 253	9/3/50	19.9
ant-E1.2	*dinglei*	18-37-20-7-4	DSDP 44	2/1/72 & 3/1/124	34.1–37.1
maj-H2	*major*	27-31-2-0-0	O-170L	surface	0
maj-P23.Q23	*major*	50-92-15-4-0	DSDP 254	1/2/20–2/2/50 (4)	1.68–2.40
maj-Q4.5	*major*	8-52-10-0-0	DSDP 264	1/1/134 & 1/6/134	0.14–0.89
min-H1	*major*	5-11-16-1-0	ALB-4693	surface	0
min-M2	*major*	10-14-6-0-0	DSDP 281	10/2/135	13.4
spB-O1	*major*	13-6-4-2-0	DSDP 318	14/3/100	24.2
min-P2	*minor*	7-17-3-0-0	DSDP 258A	6/4/100	4.76
min-Q1	*minor*	2-14-6-1-0	DSDP 208	2/4/50	1.09
mio-M1.3	*miocenicus*	5-30-1-0-0	DSDP 526A	7/2/59 & 10/1/123	7.60–8.67
mio-M2.P12.PAG	*miocenicus*	185-262-91-8-0	DSDP 516 & DSDP 516A	516: 4/2/80–12/2/80 (3) 516A: 5/2/123–11/3/CC (36)	3.75–5.62
mio-P3.5	*miocenicus*	13-42-3-0-0	DSDP 526A	2/1/125 & 3/3/50	4.68–5.49
mio-P4	*miocenicus*	17-16-4-0-0	DSDP 357	2/3/137	3.58
nud-Q1.2	*nudus*	6-7-2-0-0	DSDP 253 DSDP 254	2/2/50 1/3/50	1.90–3.33
ocu-Q1.2	*ocularis*	4-4-3-0-0	DSDP 208 DSDP 281	2/4/50 2/1/21 & 2/2/32	0.84–1.10
pan-H1	*panopsus*	4-2-0-0-0	TBD	surface (5)	0
pin-H3	*pintoi*	35-20-14-5-0	ALB-2763	surface	0
pin-P1.2	*pintoi*	10-14-2-0-0	DSDP 610A & DSDP 607	610A: 17/3/36–17/4/87 (8) 607: 12/4/88–13/5/120 (35)	2.52–3.23
pin-Q234	*pintoi*	77-109-114-79-31	CH82-24	250cm–476cm (72)	0.08–0.13
rio-P1	*pintoi*	14-13-12-3-0	DSDP 516	4/2/80	3.96
nud-M2	*praenudus*	7-11-3-0-0	DSDP 253	3/3/100	5.57
pse-O1	*pseudorobustus*	11-3-0-0-0	DSDP 549A	10/5/80	30.7
pun-Q1	*punctatus*	2-1-2-1-0	DSDP 209	1/1/75–2/2/75 (3)	0.11–1.19
rio-M1	*riograndensis*	11-7-0-0-0	DSDP 281	10/2/135	13.4
rio-M23	*riograndensis*	65-57-5-0-0	DSDP 526A	22/1/124 & 26/1/20	19.1–21.5
rio-M456	*riograndensis*	43-100-62-7-1	DSDP 526A	10/1/123–18/2/2 (5)	8.67–11.7
rob-O1	*robustus*	1-8-4-0-0	DSDP 209	15/1	34.5
rud-E1	*rudis*	12-8-4-0-0	DSDP 207A	11/4	41.4
rud-O1	*rudis*	10-10-4-0-0	DSDP 277	3/3	26.9
rud-Q1.2	*rudis*	3-13-13-4-3	DSDP 208	2/4/50 & 3/3/135	1.09–2.07
spF-E1	species 1	29-30-39-3-0	ODP 744A	14/3/147–19/4/46 (45)	30.7–35.5
spE-O12	species 2	4-35-21-7-6	DSDP 549A	7/2/80 & 8/5/80	26.1–28.1
gr1-H1.2	species 3	30-28-2-0-0	ELT47-5062 & ELT47-5064	surface	0
gr3-H1.2	species 4	36-39-5-0-0	9131–9/12 & AII-156	surface	0
gr3-P1.2	species 4	26-47-0-0-0	DSDP 610A & DSDP 607	610A: 17/2/17–17/5/23 (14) 607: 12/4/88–13/6/120 (16)	2.52–3.23
zAG-M1	*A. hazelae*	6-6-6-0-0	DSDP 526A	28/1/110	23.3
zBR-M1	*B. dictyon*	6-4-3-0-0	DSDP 516	12/2/80	5.62
zBR-H1	*B. normani*	5-0-0-0-0	multiple	—	0
zHE-K1	*H. sagitta*	5-0-0-0-0	Carnarvon Basin	—	~80

APPENDIX 2—Locality information for all samples. DSDP and ODP refer the to Deep-Sea Drilling Project and the Ocean Drilling Project, respectively. Some locality names are sampling stations of the following oceanographic research vessels: *Atlantis II* (AII), *Albatross* (ALB), *Chain* (CH), *Eltanin* (ELT), *Oceanographer* (O), and *Thomas B. Davies* (TBD). 'Map' refers to label on Figure 5 corresponding to that locality. PDWD is present-day water depth, in meters. Latitude and Longitude are in decimal form. The Carnarvon Basin locality is described by Bate (1972), Chain82–24 is discussed by Cronin et al. (1999), and the Thomas B. Davies localities are listed in Whatley and Dingle (1989).

Locality	Map	Sample type	PDWD	Latitude	Longitude
DSDP 207A	1	core	1389	−37.0	165.4
DSDP 208	2	core	1545	−26.1	161.2
DSDP 209	3	core	1428	−15.9	152.2
DSDP 253	4	core	1962	−24.9	87.4
DSDP 254	5	core	1253	−31.0	87.9
DSDP 258A	6	core	2793	−33.8	112.5
DSDP 264	6	core	2873	−35.0	112.0
DSDP 277	7	core	1232	−52.2	166.2
DSDP 281	8	core	1591	−48.0	147.8
DSDP 318	9	core	2643	−14.8	−146.9
DSDP 357	10	core	2086	−30.0	−35.6
DSDP 44	11	core	1478	19.3	−169.0
DSDP 463	12	core	2525	21.4	174.7
DSDP 516	10	core	1313	−30.3	−35.3
DSDP 516A	10	core	1313	−30.3	−35.3
DSDP 526A	13	core	1054	−30.1	3.1
DSDP 549A	14	core	2513	49.1	−13.1
DSDP 607	15	core	3427	41.0	−33.0
DSDP 610A	16	core	2417	53.2	−18.9
ODP 744A	17	core	2318	−61.6	80.6
9131–12	18	dredge	3856	20.1	−21.4
9131–9	18	dredge	4006	20.3	−21.7
AII-156	19	dredge	3459	−0.8	−32.7
ALB-2763	20	dredge	1227	−24.3	−42.8
ALB-4693	21	dredge	2089	−26.5	−105.8
Carnarvon Basin	22	borehole	—	−31.0	115.0
CH82-24	15	core	3427	41.7	−32.9
ELT47-5062	23	dredge	1404	−51.1	76.6
ELT47-5064	23	dredge	1728	−51.2	75.8
O-170L	24	dredge	2781	−30.7	156.4
TBD_2459	25	grab	300	−31.2	16.4
TBD_2690	25	grab	271	−30.5	15.8
TBD_2719	25	grab	240	−30.5	16.1
TBD_2840	25	grab	205	−30.9	15.7
TBD_6823	25	grab	120	−34.1	18.2

APPENDIX 3

Descriptions of all characters and character states in the phylogenetic analysis. Each character is followed by a list of its character states. For characters based on measured features, the range of metric values associated with each character state is listed parenthetically after each character state description. Character state descriptions are followed by notes about the character, including details on how it was measured, if appropriate. Finally, figures that describe this character or exhibit particular character states are listed. Unless specified parenthetically after the character name, the character applies to A-1 and adult instars and to both right and left valves. All multi-state characters except for characters 1 and 21 were treated as ordered. Fossae are referenced according to the labeling scheme in Figure 1.2. Muri are labeled by their bounding fossae, so for example, the mura separating the A1 and B1 fossae is referred to as the A1B1 mura.

1. Adductor muscle scar depression
   0. small, indistinct anteriorly
   1. small, completely distinct
   2. large, indistinct
   'Small' and 'large' muscle scar depressions have diameters approximately 20% and 35% (respectively) of the dorsoventral valve height.
2. Inner lamella width (Adult)
   0. relatively narrow
   1. relatively broad
   IL width was measured at the anteriormost extent of the valve. While it is difficult to measure precisely, the cutoff between the two states occurs when the IL is approximately 10% of the length of the valve. The difference between the states is most readily appreciated when specimens are viewed laterally in transmitted light: for state (1), the IL extends to the posterior edge of the AR fossae in the anterior, and to over twice the width of the posterior margin in the posterior; for state (0), the IL extends only about midway to through the AR fossae in the anterior, and no more than one and a half times the width of the posterior margin in the posterior. The inner edge of the IL can be taphonomically damaged, reducing its measured width and so care was taken to consider only specimens with an undamaged IL.
   Figure: 15.1 for state (0), 15.2 for state (1).
3. Number of pores on anterior marginal rim in the A-1 instar
   0. five pores
   1. seven pores
   The AMR is delimited by the extent of the AR1 through AR6 fossae.
   Figure: 15.3 for state (0), 15.4 for state (1).
4. Number of pores on anterior marginal rim (Adult)
   0. same as A-1 instar
   1. one pore added between A-1 instar and Adult instar near fossa AR6
   This character was defined in terms of whether or not a pore is added in the last molt so as to be independent of character 3.
   Figure: compare 15.4 versus 15.5 to see the addition of a pore near the AR6 fossa.
5. Murate pores between AR fossae (Adult)
   0. absent
   1. present
   Specimens scored as 'present' have pores on at least some of the muri dividing the AR fossae. These murate pores are not to be confused with the solate pores found at the posterior end of each AR fossae.
6. Pore at intersection of M7 & M8 fossae
   0. absent
   1. present
   This pore may be present anywhere along the intersection of M7 and M8.
   Figure: 16.1 for state (1).
7. Position of pore at intersection of M7 & M8 fossae
   0. relatively medial ($x < 0.57$)
   1. relatively posterior ($x > 0.57$)
   OTUs without this pore (character 6) were scored as unknown ("?") for this character.
   Measurement: The projected distance from the anterior termination of the M7M8 mura (LM 1), divided by the length of this mura (d). This metric increases from 0 to 1 as the position of the pore moves from anterior to posterior.
   Figure: 16.2.
8. Sieve pore on anterior side of the sulcus located anterior to the dorsal ridge
   0. absent
   1. present
   This sieve pore is usually located just posterior to a simple pore.
   Figure: 16.1 for state (1).
9. Dorsoventral position of pore in AR3 fossa
   0. located centrally in fossa ($x < 0.79$)
   1. extremely dorsal ($x > 0.79$)
   Measurement: Perpendicular distance from the pore to the ventral mura, divided by the sum of this distance plus the perpendicular distance to the dorsal mura [d2/(d1 + d2)]. This metric increases from 0 for a pore on the ventral mura, to a value of 1 for a pore on the dorsal mura.
   Figure: 16.3.
10. Position of sieve pore near fossae C6 & C7 (Adult)
    0. located anterior to the center of fossa C6
    1. located posterior to the center of fossa C6
    This sieve pore is located on the mura separating fossae C6 and C7, or on the vertical mura anterior or posterior to C6.
    Figure: 16.11 for state (0), 16.12 for state (1).
11. Position of simple pore near fossae D6 & D7 (Adult)
    0. located anterior to the center of fossa D6
    1. located posterior to the center of fossa D6
    This simple pore is located on the mura separating fossae D6 and D7, or on the vertical mura anterior or posterior to D6.
    Figure: 16.11 for state (0), 16.12 for state (1).
12. C3 fossa
    0. undivided
    1. divided
    In the 'divided' state, the position that is typically occupied by a single fossa (C3) is occupied by two fossae (see text for details).
    Figures: 4.1 and 17.3, 17.4 for state (0), 4.2, 4.3, 17.1, 17.2 for state (1).
13. Relative position of A1 & B1 fossae
    0. B1 posteroventral to A1 ($x > 2.65$ radians)
    1. B1 nearly ventral to A1 ($x < 2.65$ radians)
    Measurement: The fossa M3 is used as a reference point to judge the relative positions of A1 and B1. The angle formed by the centers of these fossae (B1-A1-M3) was used to measure their positions.
    Figure: 17.1, 17.2 for state (0), and 17.3, 17.4 for state (1).

14. Position of A6 fossa
    0. dorsal to M6
    1. dorsal to both M6 & A5
    2. dorsal to A5
    A6 was considered dorsal to a single fossa when approximately 80% or more of its area was situated dorsal to that fossa.
    Figure: 15.10 for state (0), 15.11 for state (1), and 15.12 for state (2).
15. Position of D7 fossa, relative to D6
    0. D7 positioned relatively posterior to D6 ($x < -0.75$ radians)
    1. D7 positioned relatively dorsal to D6 ($x > -0.75$ radians)
    Measurement: Angle formed by the centers of fossae D5, D6, and D7. An angle of zero indicates that the three fossae form a straight line; a negative angle indicates that D7 is located relatively posterior to D5 and D6.
    Figure: 17.7, 17.8 for state (0), 17.5, 17.6 for state (1).
16. Relative position of B2, B3, & C4 fossae
    0. C4 markedly posterior of line between B2 & B3 ($x < -0.1$ radians)
    1. C4 anterior to, or aligned with B2 & B3 ($x > -0.1$ radians)
    Measurement: Angle formed by the centers of fossae B2, B3, and C4. A negative angle means that C4 is posterior of the line formed by B2 and B3, while a positive angle indicates that C4 is anterior of this line.
    Figure: 16.4, 16.5 for state (0), 16.6, 16.7 for state (1).
17. Position of C6D6 mura, relative to C5D5 mura
    0. offset anteriorly
    1. no offset
    2. offset posteriorly
    If the C5D5 mura is followed dorsally, and the C6D6 mura ventrally, these two mura may precisely meet. Or, C6D6 may be offset to the anterior or posterior of C5D5.
    Figure: 16.8 for state (0), 16.9 for state (1), 16.10 for state (2).
18. Shape of B3 fossae (A-2)
    0. triagonal
    1. subrectangular
    Triagonal B3 fossae narrow posteriorly and insert partially between the C2 and C3 fossa. Subrectangular B3 fossae are positioned almost completely anterior to C2 and C3.
    Figure: 15.8, 15.9 for state (0), 15.6, 15.7 for state (1).
19. Width of AR7 in right valve (Adult)
    0. AR7 relatively narrow ($x < 0.55$)
    1. AR7 relatively wide ($x > 0.55$)
    Measurement: Widths of AR6 and AR7 measured where these fossae meet the AMR and the fossae to their posterior side. The metric is calculated as the average ratio of these two measurements in these two fossae (the average of d1/d2 and d3/d4).
    Figure: 18.3.
20. Position of B3, relative to C2 & C3 (Adult)
    0. B3 located anterior to C2 & C3
    1. B3 inserts between C2 & C3
    B3 was considered to insert between C2 and C3 if the mura shared by these last two fossae is approximately 20% less than of the width of C2.
21. Number of AR fossae (Adult)
    0. six in LV, six in RV
    1. six in LV, seven in RV
    2. seven in LV, seven in RV
    AR fossae are defined as those that abut the AMR from the ocular region dorsally to the intersection of the VR (or its homologue) ventrally. In all blind *Poseidonamicus* species, the number of AR fossae differs in the left and right valves: there is a small extra fossa (AR7) in the most dorsal position in right valves. Because this AR7 fossa abuts the AMR in the same region as the ocular tubercle, sighted species were considered unscorable for this character.
    Figure: 18.1, 18.2 for state (1), for state (0), note presence of only six AR fossae in the right valve of 18.6.
22. Shape of anterior field fossae
    0. fossae distinctly rounded
    1. fossae polygonal or only slightly rounded
    This character reflects the shape of the fossae in the area bounded by the mural loop posteriorly, the VR ventrally, and the AR fossae anteriorly. In addition to the rounded shape of these fossae, OTUs with state (0) have muri of the anterior field that are generally lower, broader, and more even than those of the posterior field.
23. Anterior field reticulation (Adult)
    0. primary reticulation only
    1. secondary reticulation in fossae posterior to AR, primary reticulation elsewhere
    2. secondary reticulation throughout anterior field, but primary reticulation dominant
    3. primary reticulation much reduced, with coarse secondary reticulation throughout
    4. primary reticulation completely reduced, with fine secondary reticulation throughout
    See text for a discussion of primary versus secondary reticulation. 'Coarse' secondary fossae are about 10%–20% of the size of primary fossae. 'Fine' secondary fossae are much smaller, less than 5% of the size of primary fossae.
    Figures: 9.1 for state (1), 10.2 for state (2), 9.3 for state (3), 9.4–9.6 for state (4); all other figured adults have state (0).
24. Posterior field reticulation (Adult)
    0. primary only
    1. primary reticulation of modest relief, with fine secondary reticulation
    2. primary reticulation completely reduced, with fine secondary reticulation
    See character 26 for a definition 'fine' secondary reticulation.
    Figure: 9.4 for state (1), 9.6 for state (2); all other figured adults have state (0).
25. Anterior field fossae excavation (A-2)
    0. moderately excavate primary or secondary reticulation
    1. fossae very shallow; anterior field nearly smooth
    In state (1), the fossae are so shallow as to make the entire anterior field appear smooth. In contrast to character 23, which reflects replacement of primary with secondary reticulation, state (1) of this character reflects the near absence of all reticulation in the anterior region.
    Figure: 15.6 for state (0), 15.8 for state (1).
26. Thickness of B1B2 mura, relative to A1A2 mura (Adult)
    0. B1B2 moderately thicker than A1A2 ($x < 2.2$)
    1. B1B2 much thicker than A1A2 ($x > 2.2$)
    Measurement: Each mura was measured at its narrowest point and the ratio of the B1B2 thickness to the A1A2 thickness was calculated (d1/d2).
    Figure: 17.9, 17.10 show measurement and state (0).
27. Dorsal ridge above mural loop (Adult)
    0. DR markedly thinner/absent above mural loop
    1. DR continuous above mural loop
    Reduction in the DR above the ML was considered relative to the sections of the DR anterior and posterior to the ML. In OTUs with a very reduced DR it was impossible to determine if the DR was particularly reduced above the ML. Such OTUs were considered unscorable.
    Figure: 18.4 for state (0), 18.5 for state (1).
28. Dorsal ridge posterior termination (Adult)
    0. DR terminates just posterior to D7 fossa
    1. DR terminates in broad mura extending markedly posterior to D7 fossa
    In state (1), the DR extends posterior to the D7 fossa by a distance approximately equal to the width of this fossa.
    Figure: 18.5 for state (0), 18.4 for state (1).
29. Continuity of the posterior dorsal ridge (Adult)
    0. DR continuous over ABCD fossae columns
    1. DR breaks anterior to C column, fuses medially with hingeline
    When present, this discontinuity occurs just anterior to fossa C7, at which point the DR connects to a ridge that extends medially to the hingeline. This character only considers the DR posterior to the ML, and thus is independent of character 27.
    Figure: 18.5 for state (0), 18.4 for state (1).
30. Posterior margin denticles
    0. denticles unconnected
    1. denticles connected by a thin sheet of shell material
    When present, the thin sheet of skeletal material extends outward from the dorsal margin, parallel to the commissure, and uniting the posterior denticles.
    Figure: 15.1 for state (0), 15.2 for state (1).
31. Posterior marginal rim (A-1, RV)
    0. moderately broader at the posterior extreme than elsewhere ($x < 2.2$)
    1. much broader at posterior extreme than elsewhere ($x > 2.2$)
    Measurement: This character measures the width of the posterior marginal rim at its posterior extreme, relative to its width more dorsally. The metric used is the ratio of the PMR width at the posterior extreme (d1) to its width just dorsal to a reference pore (d2).
    Figure: 19.7, 19.8 for state (0), 19.5, 19.6 for state (1).
32. Robustness of juveniles (A-1)
    0. moderate to low robustness
    1. very robust
    'Very robust' juveniles had muri that were thick and well elevated above the reticulum, with substantial among-muri variation in thickness.
    Figures: 8.3 for state (0), 11.4 for state (1).
33. Open area in the reticulum surrounding the frontal scars
    0. absent
    1. present
    This 'open area' surrounding the frontal scars arises when three fossae nearly unite into one large open and markedly excavate compartment; the

muri between these fossae are so reduced as to be nearly absent. In state (0), these fossae are as distinct as other fossae in the vicinity, and typically are not very excavate.

Figure: 19.10 for state (0), 19.9 for state (1).

34. Ocular ridge
    0. absent
    1. present

    An ocular ridge is a prominent and continuous mura that passes parallel and posterior to the AR fossae, connecting the VR to the ocular region.

    Figure: 18.6, 18.7 for state (1), all figured *Poseidonamicus* have state (0).
35. Mural bridge anterior to adductors
    0. absent
    1. present

    A mural 'bridge' was defined in Benson (1972). It consists of a rectangular box of elevated muri that surrounds and extends anteroventrally from the frontal muscle scars.

    Figure: 18.6, 18.7 for state (1), all figured *Poseidonamicus* have state (0).
36. Foveolate reticulum
    0. absent
    1. present

    Foveola were defined by Sylvester-Bradley and Benson (1971). They are superficially similar to very fine secondary reticulation, but can be distinguished by their shallowness, regular shape, and occurrence on the surface of, as well as between, primary muri.

    Figure: 18.8 for state (1), all figured *Poseidonamicus* have state (0).
37. Slope of anterior margin rim
    0. AMR flat and parallel to commissure
    1. AMR upturned at its anterior periphery

    When 'upturned' the AMR is sloped relative to the commissure such that its marginal periphery is slightly further from the commissure than its interior edge. This upturn is most pronounced in the dorsal half of the AMR.

    Figure: 19.1 for state (0), 19.2 for state (1).
38. Shape of the valves in lateral view (A-1)
    0. relatively elongate ($x < -0.04$)
    1. medium ($-0.04 < x < 0.04$)
    2. relatively high ($x > 0.04$)

    Measurement: Based on the ratio of valve height (at the adductor muscle scars) to maximal valve length. In order to increase sample sizes, both LV and RV were used; however, LVs were on average slightly less elongate than RVs. Consequently, LV and RV ratios were rendered comparable by first mean-centering all specimens for each valve separately, and then pooling these standardized ratios by OTU.
39. Shape of the anterior margin (LV)
    0. smoothly curved
    1. ventral half smoothly curving, dorsal half nearly straight

    Those specimens with state (1) have a sharp break in the anterior margin near the AR2 or AR3 fossa. Ventral to this break, the anterior margin is smoothly curving; dorsal to the break the anterior margin is nearly straight and dorsoventrally oriented, giving the anterior of the specimen a distinctively blocky appearance.

    Figure: 19.12 for state (0), 19.11 for state (1).
40. Anterior cardinal angle (Adult, LV)
    0. subdued to moderately prominent hinge ear
    1. very prominent hinge ear

    A hinge ear was considered 'very prominent' if its dorsal edge protruded from the hingeline by a distance greater than the width of the AMR.

    Figures: 8.1 and 8.4 for state (1), all other figured specimens have state (0).
41. Shape of posterior margin in lateral view (Adult)
    0. slightly caudate/subquadrate
    1. quadrate

    State assignments were operationally defined on the basis of how far posterior to the PCA the posterior margin extended. In 'quadrate' forms, the posterior extreme extends posterior to the PCA by a distance approximately equal to the width of the posterior hinge element. In 'subquadrate' forms, the posterior extreme extends approximately twice this distance. Where left and right valves differ, this character refers to left valves.

    Figures: 8.6 and 8.8 for state (1), all other figured specimens have state (0).
42. Shape of posterior region in dorsal view (Adult)
    0. posterior region increases in width immediately anterior to PMR
    1. posterior region narrows immediately anterior to PMR, then increases in width

    State (0) described the condition in which the valve increases sharply in width immediately anterior to the PMR. Specimens showing state (1) at first decrease in width immediately anterior to the PMR, and then increase rapidly in width.

    Figure: 19.4 for state (0), 19.3 for state (1).